Using an oceanographic model to investigate the mystery of the missing puerulus

Jessica Kolbusz[1], Tim Langlois[2], Charitha Pattiaratchi[1,] Simon de Lestang[3]

[1] Oceans Graduate School and the UWA Oceans Institute, The University of Western Australia, Crawley, WA 6009, Australia
[2] School of Biological Sciences and the UWA Oceans Institute, The University of Western Australia, Crawley, WA, Australia
[3] Western Australian Fisheries and Marine Research Laboratories, Department of Primary Industries and Regional Development, Government of Western Australia, North Beach, WA, Australia

Correspondence to: Jessica Kolbusz (jessica.kolbusz@research.uwa.edu.au)

Abstract. Dynamics of ocean boundary currents and associated shelf processes can influence onshore/offshore water transport, critically impacting marine organisms that release long-lived pelagic larvae into the water column. The western rock lobster, *Panulirus cygnus*, endemic to Western Australia, is the basis of Australia's most valuable wild-caught commercial fishery. After hatching, western rock lobster larvae (phyllosoma) spend up to 11 months in offshore waters before ocean currents and their ability to swim transports them back to the coast. The abundance of western rock lobster post-larvae (puerulus) provides a puerulus index used by fisheries managers as a predictor of lobster abundance 3-4 years later. This index has historically been positively correlated with the strength of the Leeuwin Current. In 2008 and 2009, the Leeuwin Current was strong, yet a settlement failure occurred throughout the fishery, prompting management changes and a rethinking of environmental factors associated with their settlement. Thus, understanding factors that may have been responsible for the settlement failure are essential for fisheries management. Oceanographic parameters likely to influence puerulus settlement were derived for 17 years to investigate correlations. Analysis indicated that puerulus settlement at adjacent monitoring sites have similar oceanographic forcing with kinetic energy in the offshore and the strength of the Leeuwin Current being key factors. Settlement failure years were synonymous with 'hiatus' conditions in the south-east Indian Ocean and periods of sustained cooler water present offshore. Post-2009, there has been an unusual but consistent increase in the Leeuwin Current during the early summer months with a matching decrease in the Capes Current, which may explain an observed settlement timing mismatch compared to historical data. Our study has revealed that a culmination of these conditions likely led to the recruitment failure and subsequent changes in puerulus settlement patterns.

1 Introduction

Fisheries management of the western rock lobster (*Panulirus cygnus*), Australia's most valuable wild-caught single-species fishery (de Lestang et al., 2018), utilizes an index of *P. cygnus* post-larvae (puerulus) settlement as one of its leading stock diagnostics. Over the past four decades, this index has been used to predict catches 3 to 4 years in advance (Phillips,

1986; Caputi and Brown, 1993; de Lestang et al., 2015), while historically being positively correlated with the strength of the Leeuwin Current (Pearce and Phillips, 1988; Lenanton et al., 1991). There was an unexpected decline in puerulus settlement numbers during the 2008 and 2009 settlement seasons (May - April). In response to this, the Department of Primary Industries and Regional Development, Western Australia (DPIRD, WA) fisheries managers made significant reductions to landings. In addition, they restructured the management system from input to output controls (Caputi et al., 2021). Puerulus settlement has subsequently recovered, but despite research regarding overfishing or possible biological and oceanographic conditions causing the change (de Lestang et al., 2015; Säwström et al., 2014), no discernible factor(s) explaining the puerulus settlement decline have been identified to date. Other research has shown that, since the recovery in puerulus numbers, there has been a latitudinal and timing shift in puerulus settlement compared to historical data (Kolbusz et al., 2021). The majority of the reduction has occurred in the first half of the puerulus settlement season (May - October; Kolbusz et al., 2021). Additionally, in the southern sites, there has been a significant reduction over the whole season. In contrast, those in the north have maintained levels of puerulus settlement during the second half of the season (Kolbusz et al., 2021).
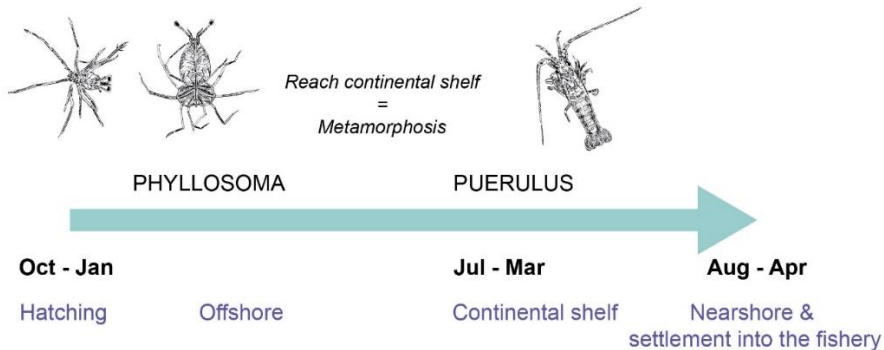
Figure 1 Early life-cycle schematic of *P. cygnus*. Below the arrow indicates each stage's approximate timing (black) and location (blue). Above the arrow displays their growth, image credit Alice Ford.

Between November and February, berried western rock lobster females release their larvae (phyllosoma) throughout the study region (Figure 1, Figure 2a). They are then transported offshore by the prevailing currents into the open ocean, where they transform through a series of temperature-dependent moults (Figure 1). They undergo their final metamorphosis into the actively swimming nektonic puerulus after approximately eight months (Figure 1). The onshore movement of puerulus across the continental shelf peaks between September and February (Phillips, 1981; de Lestang et al., 2018). Therefore, circulation patterns of the south-east Indian Ocean influence spatially varied cross-shelf transport of the puerulus (Caputi, 2008; Feng et al., 2011). After a maximum of approximately 30 days, they reach shallow areas of reef and seagrass habitats as early juveniles (Feng et al., 2011).

In the late 1960s, puerulus collectors resembling artificial seaweed were developed and deployed at several shallow-water sites within the fishery (Phillips 1981). Puerulus are currently counted at eight sites spanning the latitude of the fishery, with the centrally-located Dongara collectors (Figure 2a) now providing over 50 years of *in-situ* data (Kolbusz et al., 2021).

The puerulus settlement index (puerulus index, PI) is derived from this data, with the majority of puerulus settlement occurring between August and January(de Lestang et al., 2012). Therefore the puerulus settlement season occurs between May to April.

Research on the interaction between the physical environment and PI began in the 1980s with a strong positive relationship found between the strength of the Leeuwin Current (LC), with Fremantle Mean Sea Level (FMSL) as a proxy (Pearce and Phillips, 1988; Lenanton et al., 1991). Consequently, La Niña phases were also found to coincide with an above-average PI, thought to be due to a strengthened LC during these phases, with the Southern Oscillation Index (SOI) as an indicator of El Niño Southern Oscillation phases (Clarke and Li, 2004; Caputi et al., 2001; Pearce and Phillips, 1988). These relationships were identified through long-term correlations between the PI, FMSL, and SOI (Figure 3). Since 1988, studies have also demonstrated that the inter-annual variation in PI was influenced by the sea surface temperature (SST) and westerly (onshore) winds (Caputi and Brown, 1993; Caputi, 2008; Caputi et al., 2010). Caputi et al. (2001) defined a significant area overlapping with the spatial extent of the LC, where SST (27°–34°S, 105°–117°E) in February-April had a positive relationship with the PI of the subsequent season. The bottom temperature during the spawning season has also been identified as a cue for hatching and therefore has a possible influence on the puerulus settlement season to follow (Chittleborough, 1975; de Lestang et al., 2015).
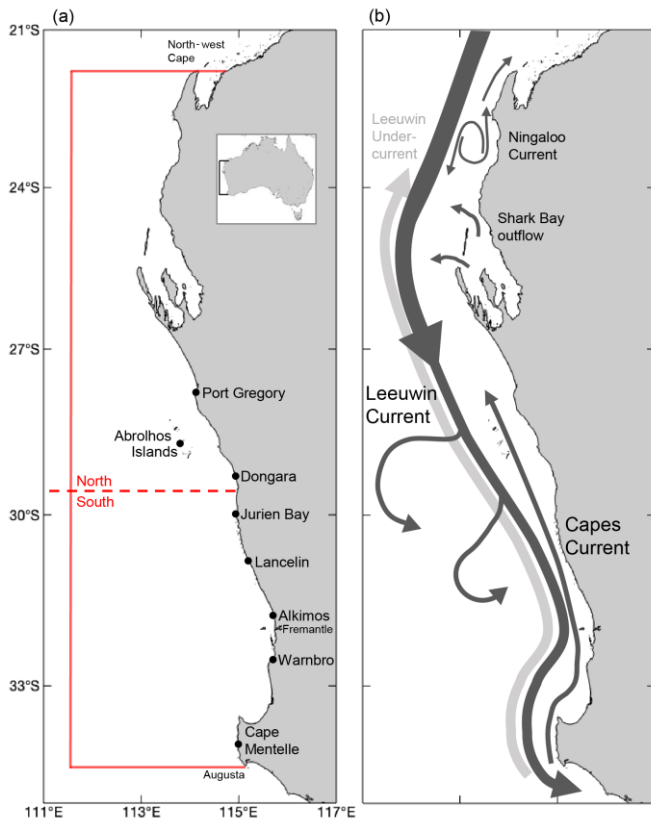
Figure 2 (a) Locations of puerulus survey sites included within this study and other locations of note. The north and south refer to the midpoint used in this analysis. In particular for kinetic and eddy kinetic energy calculation. Red boundary is the extent of

environmental variables. Inset shows location of the coastline in Australia (b) Schematic of the major currents systems thought to influence early-stage *P. cygnus* larvae movement. Relative arrow size and location show characteristic currents. Eddies generated by the LC flow down the continental shelf are also indicated.

Following the decline in the PI in 2008 and 2009 (Figure 3), the aforementioned relationships between the PI and oceanographic factors broke down (de Lestang et al., 2015; Caputi et al., 2014; Feng et al., 2011). Through one of the strongest La Niña phases on record (2011), the PI still did not recover to the previously expect high values (Boening et al., 2012; Benthuysen et al., 2014). These changes have been generally attributed to increasing water temperatures during the spawning period, resulting in an earlier onset of spawning, and a decrease in the number of storms occurring near puerulus settlement (de Lestang et al., 2015). Since this decoupling between proxy parameters and PI, additional years of contrasting settlement have been recorded, thus providing a larger dataset to re-examine these relationships following the period of low settlement.
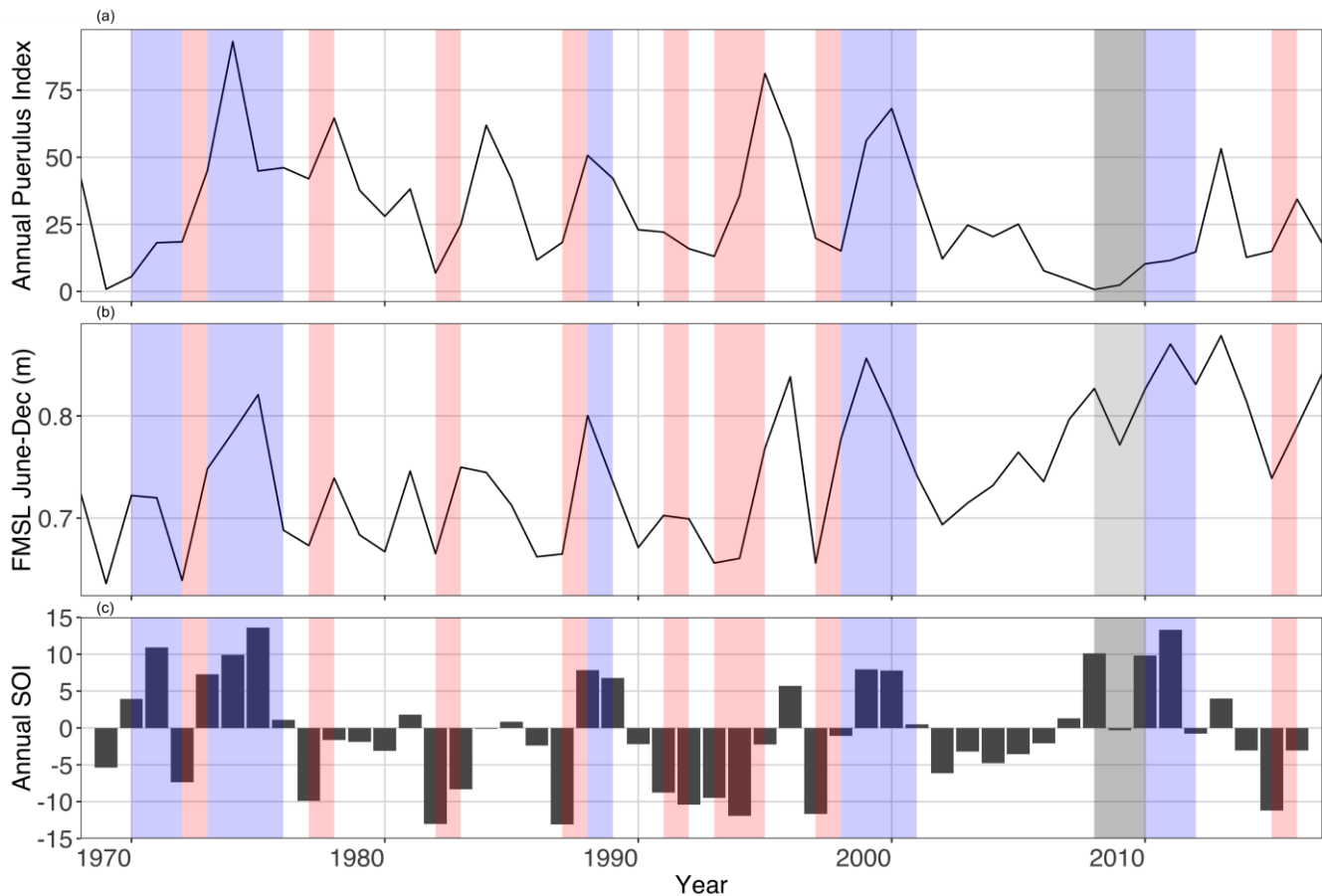
Figure 3 Time series of annual (a) fishery-wide PI (May – April); (b) Fremantle Mean Sea Level (FMSL) over June to December (m); and, (c) Southern Oscillation Index (SOI) (May –April). Grey shaded seasons indicate the less than expected PI based on a priori relationships (Caputi et al. 2001). Blue and red shading indicate a La Niña and El Niño periods, respectively. Updated to 2018 and modified from Figure 5 in Caputi et al. 2001.

90   This study aims to understand the recruitment failure and subsequent shifts in settlement patterns, particularly regarding direct physical oceanographic parameters over the 9 to 11 months before settlement. Previous research had highlighted that the causal factor of the correlation between the LC strength and PI before 2009 was unclear. Several suggestions have been made as to whether it was due to the warmer waters the LC brings, high eddy retention of larvae close to the coast, or better nutritional development within eddies (Caputi et al., 2001; O'Rorke et al., 2015; Wang et al., 2015;

95 Lenanton et al., 1991). Other parameters defining the oceanographic conditions in the region, including the northward-flowing Capes Current (CC) (Figure 2b), cross-shelf flows and the Kinetic and Eddy Kinetic energy, have been previously suggested as influencing the PI but not investigated (Hood et al., 2017; Koslow et al., 2008). The recent availability of high resolution 3D numerical oceanographic model output over an extended period (Wijeratne et al., 2018) eliminates the need to use proxies to represent oceanographic processes. Therefore, we were able to calculate directly predicated oceanographic parameters at

100 various locations throughout the fishery to investigate alongside puerulus settlement.

2 Study region

       Water circulation off the west coast of Australia is driven by the Leeuwin Current (LC) System that incorporates the Leeuwin Current, the Leeuwin Undercurrent and summer wind-driven currents, the Capes (CC) and Ningaloo (NC) currents, on the continental shelf (Figure 2b) (Woo and Pattiaratchi, 2008; Pattiaratchi and Woo, 2009). The LC is generated through a

105 meridional pressure gradient resulting from the difference between lower density water off northwest Australia and the denser water of the Southern Ocean (Hamon, 1965; Pattiaratchi and Buchan, 1991; Pearce and Phillips, 1988). The mean southward volume transport of the LC peaks around 32.8⁰ S due to South Indian Counter Current input (Wijeratne et al., 2018). Near 28⁰S statistical analysis has shown a break-point in the LC, suggesting responses from the current's forcing along the coastline may differ on either side of this latitude (Chittleborough, 1976; Berthot et al., 2007). The El Niño Southern Oscillation (ENSO)

110 cycle causes the pressure gradient to decrease/increase during an El Niño/La Niña episode, resulting in a weaker/stronger LC and cooler/warmer sea surface temperature SST (Pattiaratchi and Buchan, 1991; Feng et al., 2003; Wijeratne et al., 2018). This is supported by strong correlations between the Southern Oscillation Index (SOI as an indicator of ENSO phases) and LC transport at 34⁰ S with a 6-month lag (Schiller et al., 2008).

       The LC is stronger during austral winter (May – July) and weaker during the austral summer (November- March) due

115 to variations in the equatorial wind stress and the Australasian monsoon season (January – March) (Pattiaratchi and Siji, 2020; Pattiaratchi and Woo, 2009; Smith et al., 1991; Wijeratne et al., 2018). A weaker secondary peak in the LC also occurs over December/January (Wijeratne et al., 2018). During the summer months, southerly wind stresses overcome the alongshore pressure gradient, moving upper layers offshore and favouring upwelling onto the continental shelf (Pearce and Pattiaratchi, 1999). The CC can be identified through cooler waters initiated around 34⁰ S with the cooler water extending to 27⁰ S inshore

120 of the LC (Figure 2b) (Gersbach et al., 1999). The LC migrates offshore and is weaker over these sea-breeze dominated summer

months, whereas, during winter, it floods the shelf and dominates the distribution of water masses (Cresswell et al., 1989; Pattiaratchi et al., 1997; Woo and Pattiaratchi, 2008).

Mesoscale eddies have been identified in the LC system for more than 30 years (Andrews, 1977; Pearce and Griffiths, 1991; Cosoli et al., 2020). The LC, and its associated flows, become unstable with the significant variations in topography over the latitudinal extent of the current, generating eddies, meanders and offshoots (Batteen et al., 2007). Therefore, as the LC strength increases, the system becomes more unstable, causing kinetic energy to increase (Feng et al., 2005; Pattiaratchi and Woo, 2009). The Abrolhos Islands at 28.8º S and the narrowing of the continental shelf slope south of Dongara and the Perth Canyon are major topographic features for the preferential generation of these eddies (Figure 2b) (Feng et al., 2005; Meuleners et al., 2008; Rennie et al., 2007; Huang and Feng, 2015; Cosoli et al., 2020). They have a mean radius of ~100 km and generally keep their original formation shape, lasting approximately eight months (Fang and Morrow, 2003; Cosoli et al., 2020).

3 Methods

3.1 Puerulus settlement data

Puerulus settlement is surveyed year-round, currently at eight sites across the fishery (between 34 - 27°S) using artificial seagrass-like collectors (Figure 2a). Sampling is conducted as close as possible to the full moon but may occur five days on either side. Therefore, puerulus are likely to have settled on the previous new moon period, giving approximately monthly data (de Lestang et al., 2012). The monthly puerulus settlement at each site is calculated as the average number of puerulus per collector. For this study, we used the puerulus settlement data from 2001/02 season to 2016/17 at each of the eight sites (Figure 2), aligned with high-resolution oceanographic data hereafter detailed and estimates of western rock lobster spawning biomass. Puerulus settlement data for each site was split into "Early" (May – October) and "Late" (November – April) portions, as described by Kolbusz et al. (2021).

3.2 Oceanographic data

To explore the variation in puerulus settlement, alongside the prevailing oceanographic conditions, a single value for the respective early or late portion of the season was determined. Where relevant, the oceanographic variable was the same for both portions.

3.2.1 Numerical model outputs

The Regional Ocean Modelling System (ROMS) has been used in hindcast mode (past-time) for the whole of Australia (ozROMS) to resolve subsurface and surface currents and the associated volume transports (Wijeratne et al., 2018). This is a fully three-dimensional circulation model, resolving processes along the continental shelf, including tides, setting it apart from other ocean models for the same region. The grid was set at a horizontal spacing of 3 km to allow for topographic

detail, providing predicted water movement. At the time of writing, ozROMS model output was available for the period 2000-2017. Details and validation of the model are described by Wijeratne et al. (2018). Examination of this predicted data set allows for the strength of the Leeuwin Current (LC), Capes Current (CC), and cross-shore transport to be determined, as well as estimates of kinetic (KE) and eddy kinetic energy (EKE) (Pattiaratchi and Siji, 2020). Their fluctuation is indicative of the conditions off the west coast of Australia.

Monthly surface KE and EKE was calculated from ozROMS to characterize the variability in the currents. A monthly time series was estimated following Eq. (1) for KE and Eq. (2) for EKE:

$$KE = \sqrt{\frac{u^2 + v^2}{2}},$$ (1)

$$EKE = \sqrt{\frac{u'^2 + v'^2}{2}},$$ (2)

where u and v are the monthly mean meridional and zonal velocities, respectively (Caballero et al., 2008), and u' and v' are the monthly averages with the climatological means subtracted to remove seasonality (Luo et al., 2011). The months that phyllosoma are offshore, depending on when they have hatched, can be between October (year – 1) to March (year + 1) (Figure 2). Therefore, the calendar year from January to December was used to obtain an average for the offshore conditions spanning the possible time frame offshore. Due to different mean oceanographic conditions, we considered a north and south offshore box (Figure 2a) that covered the approximate extent of where phyllosoma are transported (Feng et al., 2010; Berthot et al., 2007; Feng et al., 2011). For our analysis, we have not defined the directionality and size of eddies. Still, it is an important consideration pertinent to larvae energy stores that would require further modelling outside the scope of the current study (Cetina-Heredia et al., 2019b).

The monthly transport estimates of LC and CC (in Sverdrups, Sv = 10^6 m^{3}s^{-1}) were derived using the ozROMS hindcast dataset (Wijeratne et al., 2018). The transport for each current was defined as follows: (1) CC as northward volume transport of water across latitudes 27°S, 30°S and 34°S in water depths less than 100 m; and, (2) LC as southward volume transport of water across latitudes 27°S, 30°S and 34°S but in water depths greater than 100 m but limited to upper 300 m of the water column (Table A1, Appendix A). For the LC austral winter strength, the transport over June, July and August was averaged, and for summer, December, January and February were averaged. The LC summer period corresponds to recently hatched larvae (spawning season, s -1) leaving the continental shelf and puerulus returning in the "Late" portion of the season (settlement season, s) (Figure 2). The LC winter period corresponds to when puerulus are returning to the shelf (settlement season, s). The CC strength was divided into early (September, October and November) and late (December, January, February and March) and corresponded to the time when recently hatched larvae were leaving the continental shelf (spawning season, s -1) and puerulus returning in the "Early" and "Late" portions of the settlement season respectively (Figure 2).

Cross-shelf transport (in Sv) was calculated for each monthly time step between the depth contours (200 – 50 m) over 2 degree latitudinal bins (26 - 28º S, 28 - 30º S, 30 - 32º S and 32 - 34º S) (Table A1, Appendix 1). These latitudinal bins were

chosen closest to account for differences in topography and cross-shelf flow differences across the survey sites. Monthly averages for each latitudinal bin indicated that the variability in transport is highest over April to September. These months correspond to the eastward "on" movement of puerulus. Recently hatched larvae cross the shelf (westward, "off" in the spawning season) to the open ocean between September and March (Figure 2). These two sets of months were averaged to get values of cross-shelf transport (as phyllosoma "off" and as larvae "on") for each season (Figure 2).

Temperatures in the model layer immediately above the seabed ('bottom temperature') over the spawning depths (40 – 80 m) were retrieved from ozROMS due to the absence of in-situ data (de Lestang et al. 2015). The predicted values were averaged over a northern and southern subset (Figure 2a) of the whole spawning season (September - March). Due to the ozROMS hindcast starting in 2000, values were only available from the 2001 season since the spawning season is the calendar year prior to settlement. Despite de Lestang et al. (2015) using monthly values, we found only a small amount of variation between the months and therefore used a single bottom temperature value to represent a season. The temperature in the top 100 m of the water column, east of 108ºE, as a mean annual value from ozROMS was also included. This accounts for temperature variation over the migrating depths phyllosoma occupy over their early pelagic life-cycle (Griffin et al. 2001; Feng et al. 2011).

3.2.2 Satellite-derived sea surface temperature (SST)

Satellite-derived SST data for the study region were obtained from the Integrated Marine Observing System (IMOS) Australian Ocean Data Network (AODN) portal (portal.aodn.org.au). The climatology data, centred on the base period 1993 – 2020, SST Atlas of Australian Regional Seas (SSTAARS) (Wijffels et al., 2018) were used to derive monthly SST anomalies for the region extending offshore to 108ºE (extent in Figure 2, see also (Pattiaratchi and Hetzel, 2020)). This was to reflect the extensive duration (~9 months) of the pelagic larval and pre-settlement stage *of P. cygnus* (Phillips, 1981). All monthly SST anomalies were initially included in the analysis due to the likely importance of temperature on all stages of the pelagic larval stage (Caputi et al., 2001; de Lestang et al., 2015).

3.3 Independent Breeding Stock Survey (IBSS)

Independent Breeding Stock Surveys (IBSS) have been conducted annually since 1992 over the last new moon (~ 15 November) before the start of the fishing season (de Lestang et al., 2018). The catch rates of spawning females from this survey (adjusted for fecundity) provide a standardized egg production index. It is conducted at up to six sites spanning the fishery and close to the peak in egg production (November) (Caputi et al., 1995; Chubb, 1991; de Lestang et al., 2016). Therefore, IBSS was included in our analysis, accounting for variability in the number of hatching larvae.

3.4 Generalized Additive Modelling

The oceanographic variables likely to influence water movement and the distribution and survivorship of *P. cygnus*, detailed above, were considered as predictors of the puerulus settlement within a generalized additive model (GAM). In

addition, the IBSS was included as a predictor to include variability in the number of hatching larvae. Due to the extensive latitudinal range of the settlement data, some environmental variables were dividing into northern, central or southern areas depending on the data type and availability. A value was obtained for each possible predictor variable to align with each half of the puerulus season (Appendix A, Table A1). Firstly, linear regression analysis was performed to assess whether strong (>0.70) correlations existed between variables. Where valid, a case by case approach was taken to determine whether both, an average, or one of the two variables was included in the overall model before the time series modelling - this eliminated potential problems with collinearity and overfitting (Graham, 2009). Bottom temperatures were all highly correlated (>0.89) and therefore averaged to give a single variable. Co-correlation between the SST of adjacent months lead to a winter and summer average being used.

GAMs with full subset model selection (FSSgam) were used to investigate the influence of the final 16 (8 eights, early and late settlement periods) different response variables (Fisher et al., 2018). Predictors were initially limited to a maximum of three knots per spline. However, due to the relatively small sample size and heterogeneous distribution of the predictors, cross-shelf transport remained, but other predictors were treated as linear relationships. Model sizes were limited to three predictors to prevent overfitting. Model selection was based on Akaike's An Information Criterion (AIC, Akaike, 1973) optimized for small samples sizes (AICc, Hurvich and Tsai, 1989). The best models selected were the most parsimonious within two AICc units of the model with the lowest AICc (Burnham and Anderson, 2002). Importance scores for each variable were obtained by summing the AICc weights of each model that each variable occurred within (Fisher et al., 2018).

The data for each oceanographic and meteorological variable were collated into annual values. They resulted in a total of 39 possible predictors of the late puerulus settlement (8 sites) and 33 possible predictors of the early puerulus settlement at sites (8) (Appendix A, Table A1). LC strength in summer and the late CC strength predictors for early settlement were omitted since they occur after early settlement each season. Considering the large number of predictors and interpretation of the results, a hypothesis table including each predictor was made (Table 1). Given that the predicted data availability and the spawning season is in the calendar year prior, the relationship between all predictors and puerulus settlement was limited to the 2001 to 2017 seasons.

The R language for statistical computing (R Core Team 2018) was used for all data manipulation (Wickham et al., 2018) (dplyr, Wickham et al. 2018) and analysis (Wood, 2017) (mgcv, Wood 2011). In addition, MATLAB and the m_map toolbox were used for any spatial plotting (MATLAB, 2019b; M_Map: A mapping package for MATLAB, Version 1.4m).

3.5 Exploration of oceanographic patterns

Findings of importance were expanded on from the results of the generalized additive model (GAM) analysis. Seasonal and inter-annual variability, not captured within the GAM, were explored. An extended period of low activity was experienced in the south-east Indian Ocean between 2001 and 2007 (Pattiaratchi and Siji, 2020). Given that processes in the ocean do not respond instantaneously, these 'hiatus' conditions were explored as a whole. ENSO information (SOI) and the

Fremantle Mean Sea Level (FMSL) was obtained from the Bureau of Meteorology (Bureau of Meteorology, 2021a, b). Altimeter data was accessed from the IMOS AODN to investigate the relationship between the PI and the energy system, in particular, the long-term KE and EKE over the south-east Indian Ocean (Pattiaratchi and Siji, 2020)

250 During the summer, the interactions between the Capes Current and Leeuwin Current were also addressed (Pattiaratchi and Woo, 2009). First, the LC and CC summer period strengths were standardized for each season, and then the difference between the two was plotted alongside the early and late puerulus settlement levels.

255 **Table 1 Predictor variables and metrics used in multiple regression to investigate variability in puerulus settlement and subsequent hypothesis. The subscript *s* identifies the relativity of a month to the puerulus settlement season (May - Apr) in question. *s - 1* is within the season prior and *s + 1* is after. –ve denotes negative relationship and +ve denotes and positive relationship.**

Predictor variable	Metric used	Hypothesized relationship to puerulus settlement
Leeuwin Current (LC)	Southward strength of the current in Sverdrups (Sv) at northern, central and southern locations for three periods: **1**.Larvae hatching / transport offshore (Dec_{s-1} - Feb_{s-1}). **2**. Puerulus transport towards continental shelf (May_s - $June_s$) **3**. Peak settlement (Dec_s - Feb_s).	**1**. -ve (all sites). **2**. +ve (all sites). **3**. -ve (north sites), +ve (south sites).
Capes Current (CC)	Northward strength of the current in Sv at a north, two central and a south location over two periods: **1**.Larvae hatching / transport offshore (Sep_{s-1} - Nov_{s-1} (early) and Dec_{s-1} - Feb_{s-1}(late)) **2**.Peak settlement (Sep_s - Nov_s(early) and Dec_s - Feb_s(late))	**1**. +ve (all sites) **2**. +ve (north sites), -ve (south sites)
Kinetic and eddy kinetic energy	Kinetic and eddy kinetic energy of the south-east Indian Ocean in cm^2/s^2 over a north and south area defined in Figure 2a. **1**. phyllosoma offshore (Jan_{s-1} - Dec_s)	**1.** +ve (all sites)
Cross-shelf transport	Cross-shelf transport over the continental shelf (150 - 50 meters) in Sv over a northern, two central and southern latitudinal bins. **1**.Larvae hatching / phyllosoma transport west (Sep_{s-1} - Mar_{s-1}) **2**.Puerulus transport east (Apr_{s-1}- Sep_s)	**1**. Westerly (-Sv) +'ve **2**. Westerly (+Sv) -'ve
Temperature	Water temperature over three periods. **1**. SST summer (Sep_{s-1} - Mar_{s-1}) and SST winter (Apr_{s-1} - Aug_s) **2**.Bottom temperature during spawning (40 - 60 m depth, Sep_{s-1} - Mar_{s-1}) **3**.Top 100 m Early-stage phyllosoma. (Jan_{s-1} - Dec_s)	**1**. SST +ve (all sites) **2**. -ve (all sites) **3**. +ve (all sites)
Independent Breeding Stock Surveys (IBSS)	**1.** IBSS index for the spawning season	**1.** +ve (all sites)

4 Results and Discussion

Results and discussion are combined into three sections (1) time-series exploration of *P. cygnus* settlement between 2001 and 2017 and associated oceanographic conditions experienced by the larvae to represent each puerulus settlement season (May to April); (2) exploring the correlation of oceanographic conditions with settlement data through a general additive model analysis, and (3) inter-annual and seasonal oceanographic variability.

4.1 Time-series patterns

Puerulus settlement differs dramatically over the latitudes of the fishery, with central latitudes experiencing the highest numbers (Figure 4). At the Abrolhos (Figure 4a), the late settlement is consistently higher and remained consistent after the recruitment failure, which is expected (Kolbusz et al. 2021). Other sites display similar early and late puerulus settlements before 2008. However, after 2009, recovery occurs predominately in the latter half (Figures 4a, c, d and e).

Figure 4 panels (a) through (h) showing monthly average puerulus counts
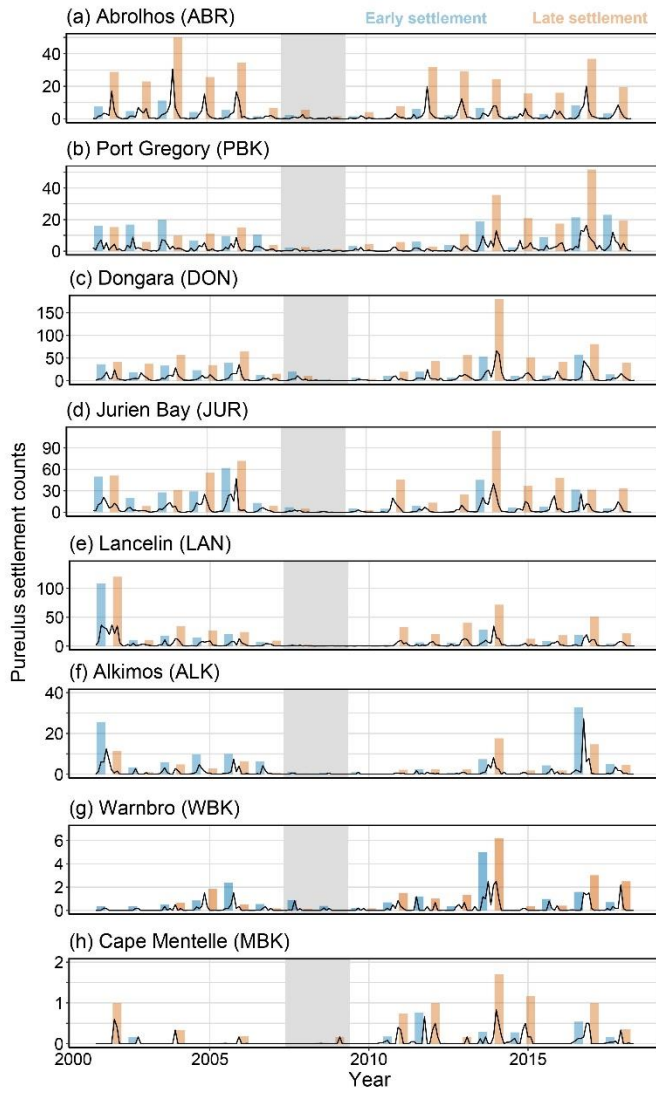
Figure 4 Monthly average puerulus counts for each monitoring site (black line) with the early (May - October, blue) and late (November - April, red) puerulus settlement for the season. The index is a sum of the included monthly average puerulus counts. Grey shaded seasons (2008 and 2009) indicate the less than expected PI based on a priori relationships (Caputi et al. 2001).

The three temperature variables (SST, top 100 m temperature and bottom temperature) all followed a similar pattern to one another (Figures 5 a-c). They gradually decreased from highs in 2000 to a low in 2005 before slightly increasing from 2008, all reaching maxima in 2011 when a marine heatwave occurred in February (Wernberg et al., 2012). A decrease of approximately 1-2°C in bottom temperature during the spawning season was evident over the early 2000s, which shifted over the low PI seasons (grey seasons, Figure 5 a-c). It then increased again by 2012 (Figure 5). Until the heatwave, the variation in PI at some sites (Lancelin and Port Gregory) additionally aligned with the SST fluctuations. This is likely the bottom

280 temperature variation captured by de Lestang et al. (2015). The winter months (June to August) had less than one degree of between year annual variability over the entire temporal scale.
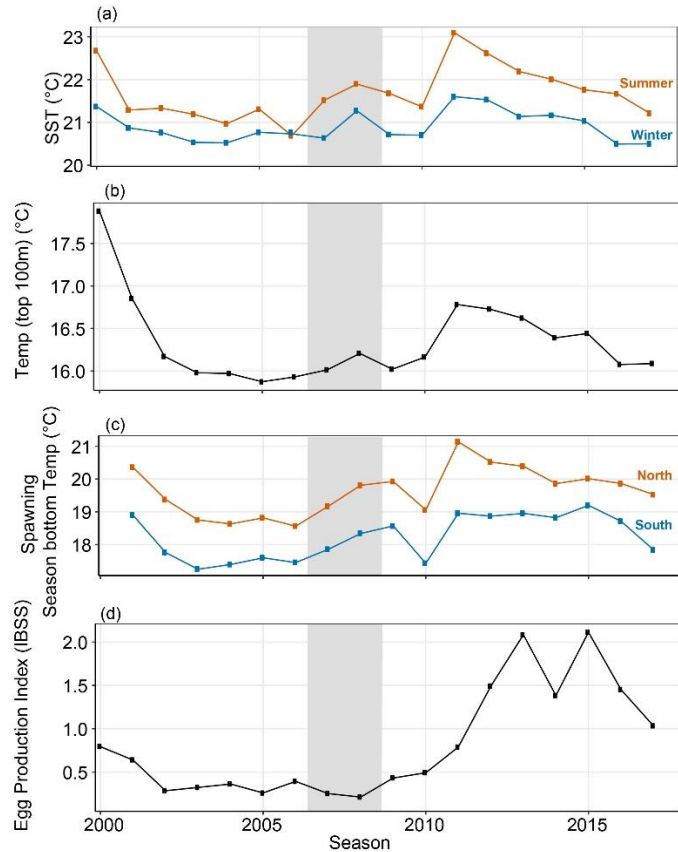
Figure 5 Parameters calculated for seasonal analysis of PI (a) Sea surface temperature (°C) from 24 - 34° S and out to 108° E obtained from the SSTAARS daily dataset on the IMOS AODN portal from 1996 to 2016; (b) Temperature in the top 100 m of the offshore
285 **area from 24 - 34° S and east of 108°E over Jan - Dec, the average time phyllosoma are offshore (c) Average bottom temperature (40 – 80 m depths) (°C) of the spawning season for associated PI season for October to March in the northern (blue line, shown in Figure 2a) and southern latitudes (red line, shown in Figure 2a) of the fishery (d) The Independent Breeding Stock Survey Index (IBSS) lagged one year to give a spawning stock index for the year prior (de Lestang et al. 2016). Grey shaded seasons (2008 and 2009) indicate the less than expected PI based on a priori relationships (Caputi et al. 2001).**

290   The IBSS was consistently under 0.5 from 2002 until the 2011 season before increasing three-fold by 2013 to record-highs (Figure 5) (de Lestang et al., 2016). Previous studies have not found the IBSS to be implicated in the recruitment failure (de Lestang et al., 2015). However, it was included in the current analysis for completeness and because studies of recruitment failures in other fisheries have frequently suggested spawning biomass to be a factor (Guan et al., 2019; Ehrhardt and Fitchett, 2010). In addition, the IBSS increased from 2011; this is likely due to the restrictive fisheries management. After the lower

295 than expected puerulus settlement in 2008 and 2009, restrictions to fishing were designed to preserve spawning biomass. Therefore the IBSS was expected to increase.

The LC was the strongest over the winter months, reaching 7 Sv in the 2000 season at 34º S (Figure 6a). However, the summer LC was strongest in 2010, at 27º S. Both values align with strong La Niña conditions (Boening et al., 2012). This maximum, however, did not correspond to a maximum in winter LC strength (Figure 6b) (Wijeratne et al., 2018). Over the initial months of the CC forming (Figure 6c), it is, on average, strongest at 30º S. The CC displayed a roughly a similar pattern across all latitudes with less variability in current at 27º S where it is weakest (Figure 6 c and d). CC minima occur over the 2010 to 2012 seasons in the early and late strength signals (Figure 6 c and d). Spatial variations in the LC and CC were distinguishable with increased LC at the southern latitude (Figure 6 a and b) and the strongest CC signature at 30º S (Figure 6d) as reported previously by Wijeratne et al. (2018).
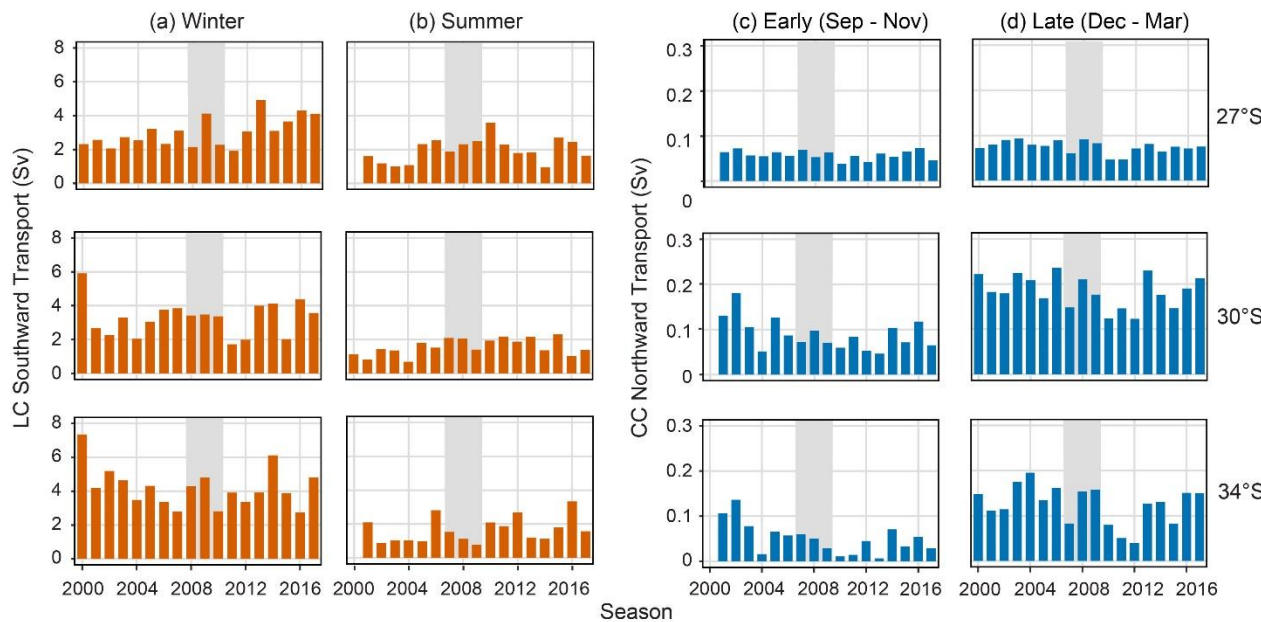
Figure 6 Leeuwin (LC) and Capes Current (CC) strengths at 27º S, 30º S and 34º S (a) LC (southward transport, Sv) over winter (May - July) and (b) summer (December - February) (c) CC (northward transport, Sv) (c) over the early portion of the summer (September - October) and (b) late portion of the summer (December - March). Grey shaded seasons (2008 and 2009) indicate the less than expected PI based on a priori relationships (Caputi et al. 2001).

Water circulation at all latitudes of the fishery were predominantly driven by the LC with the changing topography down the coast causing less onshore flow on average within the centre of the fishery (29º S) (Rennie et al., 2007; Feng et al., 2010; Wijeratne et al., 2018). Regions with a wider continental shelf generally have higher retention of waters, therefore, causing less cross-shelf transport of water. Depth-averaged cross-shelf transport of water was predominantly onshore at both 33°S and 29°S (Figure 7). This was not unexpected given the steep topography of the continental shelf and LC interactions. Average monthly variations in cross-shelf transport indicated that between April and September, onshore transport increased at 33°S and 29°S, however, decreased at 31°S and 27°S (Figure 7). Coastal geographic features increase the spatial heterogeneity over the latitudes and how the LC interacts with the nearshore (Feng et al., 2010). At 27°S, on average offshore

transport was possibly due to more mixing and a wider continental shelf. This is due to the topography of Shark Bay and the

320   contribution of the Ningaloo Current (Figure 2b), likely playing a role (Woo and Pattiaratchi, 2008).
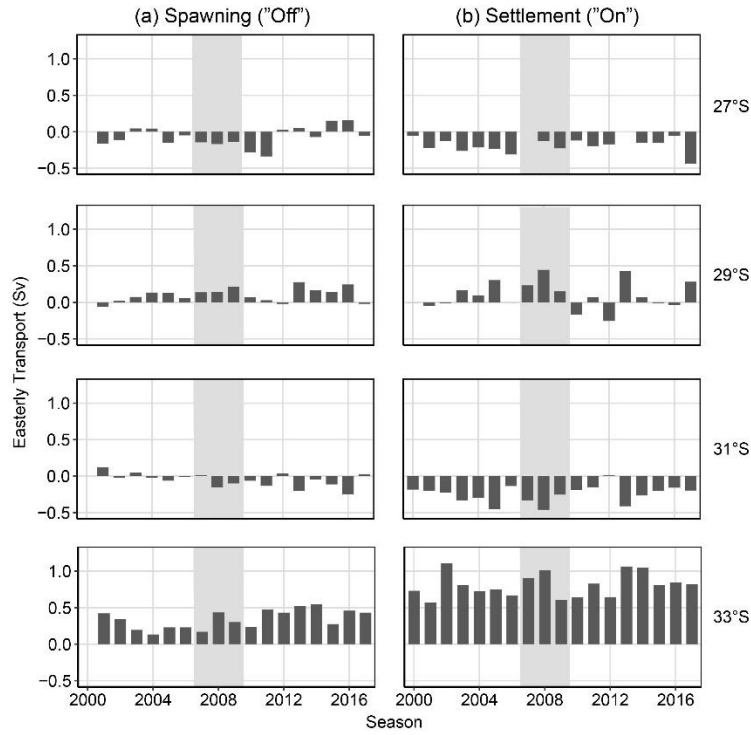
Figure 7 Cross-shelf transport (easterly) between 200 - 50 meters over 2-degree latitudinal bins (26-28º S, 28-30º S, 30-32º S and 32-34º S). Averaged for the (a) spawning "off" transport season (September-February, season -1) and (b) settlement "on" transport season when variation in cross-shelf transport is the highest (April-September). Grey shaded seasons (2008 and 2009) indicate the
325   **less than expected PI based on a priori relationships (Caputi et al. 2001).**

Variations in EKE and KE over the time series show approximately 5-yearly patterns (Figure 8) in fluctuation with maxima in 2000, 2005 and 2011 aligning with ENSO events (Pattiaratchi & Siji 2020). From 2002 to 2008, the KE and EKE were relatively low, indicating a weaker LC over those seasons. Particularly over the southern box, the decrease in KE and EKE and recovery by 2012 show similar patterns to the puerulus settlement (grey years, Figures 8c and d). Additionally, the

330   southern box shows increased variability, suggesting greater variability in the LC at southern latitudes (Figures 8c and d). Conversely, the northern values, particularly for KE, increased over the same time frame, with less variability (EKE), indicating that different forcing mechanisms, such as the South Indian Counter-Current, may play a role (Figures 8c and d).
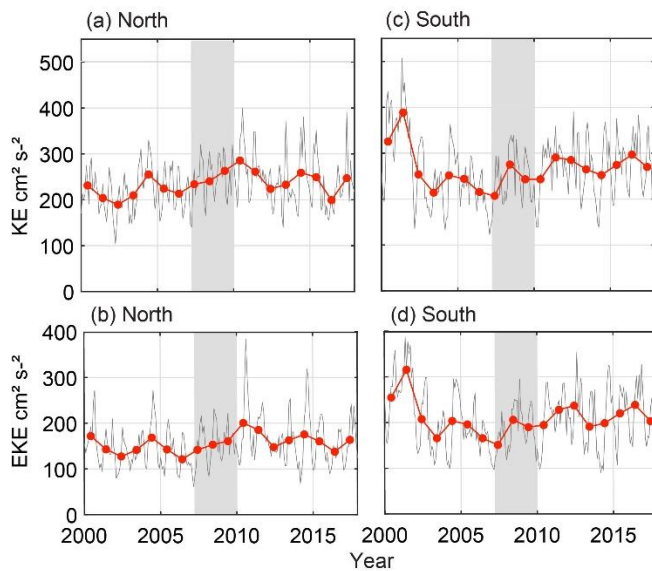
Figure 8 Monthly kinetic energy and eddy kinetic energy (grey) with yearly averages (January-December) (red). North and south divide are shown in Figure 2a. (a) KE (cm^2 s^{-2}) in the north (b) EKE (cm^2 s^{-2}) in the north (c) KE (cm^2 s^{-2}) in the south (d) EKE (cm^2 s^2) in the south. Grey shaded years (2008 and 2009) indicate the less than expected PI based on a priori relationships (Caputi et al. 2001).

4.2 Generalized Additive Model

The generalized additive model (GAM) analysis shows that puerulus settlement at adjacent sites tend to be influenced by similar oceanographic variables. However, the Abrolhos (northern-most and offshore) and Cape Mentelle (southern-most) sites are unique (Figure 9, Appendix B). The most significant relationships did vary between the early and late portions of the seasons and between sites, as expected (Table 1). Those of note are discussed hereafter.

In contrast to our predictions (Table 1), sites were correlated by a negative relationship to KE in the north for early settlement (Figure 9a). This correlation was more robust for the northern sites. A strong KE implies a strong LC signature over the defined spatial area (Figure 2a). Comparatively, EKE and KE in the south had positive relationships to sites in the centre of the fishery for early and late settlement, suggesting a different forcing could be at play (Figure 9). This was alluded to within the time-series analysis (Figure 8). The possibility that two adjacent parts of the south-east Indian Ocean would have opposing effects on the settlement at only two locations appears spurious. However, the southern and central flows of the South Indian Counter Current (sSICC, cSICC) flow eastward within the southern and northern KE 'boxes' respectfully (Menezes et al., 2014). These current jets connect with the LC and may cause the temporal and spatial difference in KE and subsequent influences on puerulus settlement. In particular, for the Abrolhos, KE in the north is within the most parsimonious model for early and late settlement. Due to the sites' location offshore, increased water movement may prevent puerulus from successfully settling on the islands within the defined area of KE. Instead, they could swim elsewhere with less resistance.

This difference in KE relationships suggests different driving mechanisms over the fishery on both the temporal (early and late) and spatial (north and south) scale.
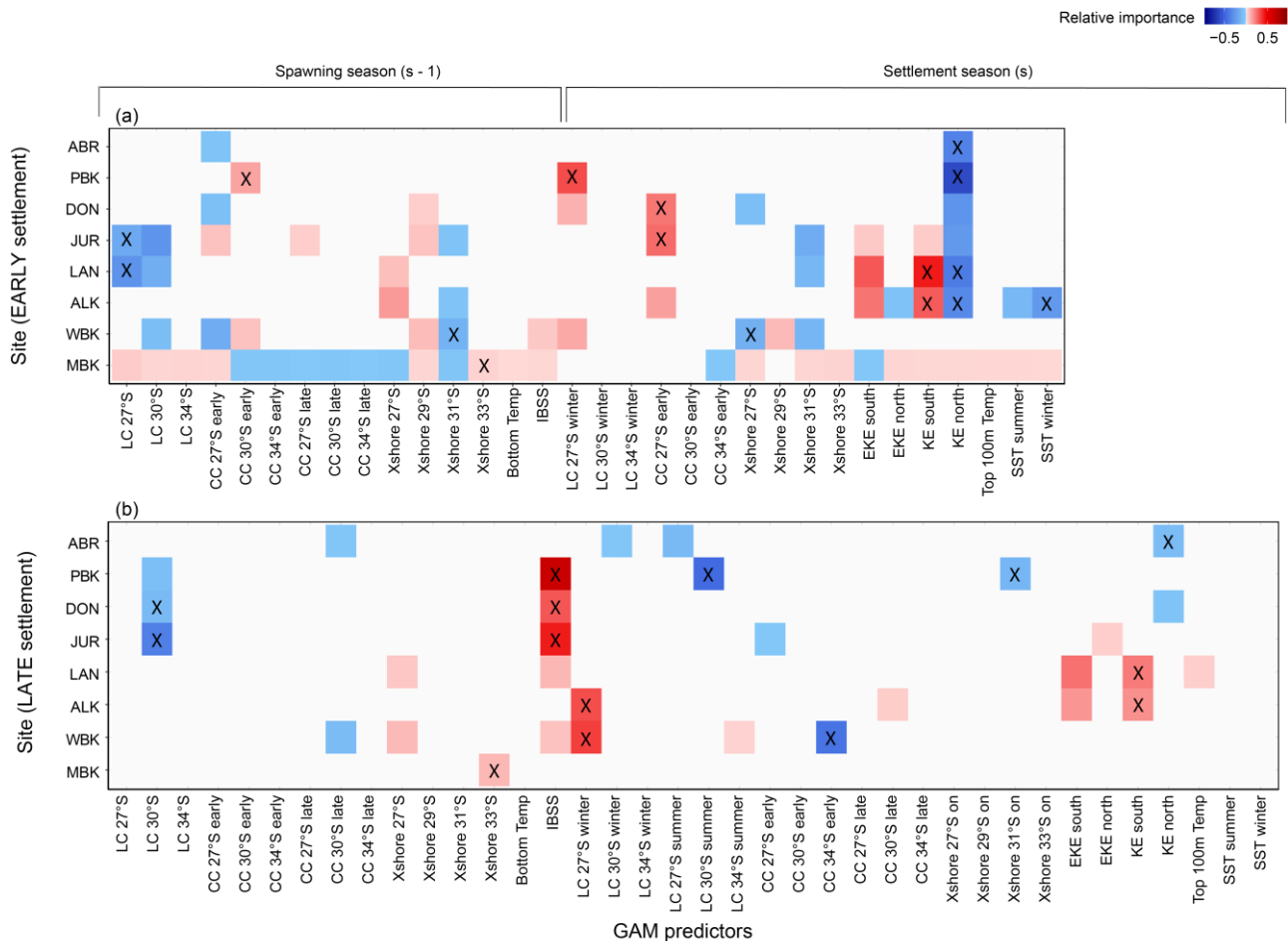
Figure 9 Variable importance scores within 2 AIC of the top model from the multiple linear regression analysis (GAM) to predict the (a) early and (b) late settlement at sites. Full results are in Appendix Table B1 (early) and B2 (late). The timeline (above) indicates the timing of the variables from either the spawning season (s-1) where larvae are moving offshore (westward) and the settlement season (s) where larvae are moving eastward. Positive (red), zero (white) and negative (blue) relationships with variables are shown, and variables within the most parsimonious model for each site are indicated (X).

The model results provide clues regarding the influence of the LC and CC (LC winter, LC summer, CC early and late) on phyllosoma when they are in later-life stages. Interestingly, the LC during the spawning season at 27⁰ S was within the most parsimonious model for Lancelin early settlement as a negative relationship (Figure 9a). Thus, for Lancelin, the LC may have been too strong for some early-stage phyllosoma to cross the shelf, to get westward, without being swept too far south for survival. Especially given the steep continental shelf at this latitude. In winter, a stronger LC (puerulus reaching the

continental shelf) and a stronger CC (puerulus settling on reefs) were suitable for early settlement at Dongara. This was a hypothesized result (Table 1) and was also consistent at adjoining sites (Port Gregory for LC and Jurien Bay for CC, Figure 9a) (Pearce and Pattiaratchi, 1999). For later settlement, the opposite relationships occur. The LC in summer has a negative relationship to Port Gregory (and Abrolhos), and the CC has a negative relationship with Warnbro (Figure 9b). This was

375   expected for Port Gregory, a northern site, to be negatively influenced by the southward-flowing current (LC), transporting puerulus further southward. Similarly, southern sites are negatively influenced by the northward-flowing current (CC), transporting puerulus northward. However, these trends become vague over the central latitudes of the fishery where little to no relationships are found, especially during the summer of hatching (Figure 9a, CC 27° S early). This draws attention to the spatial and oceanographic heterogeneity of the study sites. Given the mix of expected and unexpected and strong and weak

380   results from the multiple regression analysis, particularly for the early settlement, it is clear complex forcing's are at play in the system, with both currents flowing in opposing directions perpendicular to the direction puerulus are swimming. The influence of factors found to have the strongest correlation on puerulus settlement is presented in the following section (4.3).

       The IBSS shows a strong positive relationship with Port Gregory, Dongara, Jurien Bay, Lancelin and Warnbro over the late settlement. However, it has little relationship with the early settlement (Figure 9 a and b). Nevertheless, these positive

385   relationships corroborate that the egg production influences the number of larvae returning to the coast as puerulus and may more accurately represent the spawning stock of puerulus reaching the coast over the latter half of the settlement season. Given the longer time series available for the IBSS and Dongara settlement, we reanalyzed the relationship for a more extended period. We found that pre-2000 that IBSS is a reasonable predictor with an R^2 of 0.434 and explaining 30.3% of the deviance in the Dongara settlement (Figure 10). In an ideal scenario, one would expect all sites, both early and late, to have a relationship

390   with the spawning stock. For locations where increased IBSS did not positively correlate with PI, it may be solely that the influence of oceanographic factors on the puerulus settlement was more substantial.

       Cross-shelf transport shows irregular patterns between the sites. Cross-shelf transport for the spawning season (27° S, 29° S and 33° S, Figure 9a) has some positive links to increased settlement in the early half of the season for sites south of Dongara. However, this is the opposite for 31° S (Figure 9a), but these relationships are less pronounced over settlement later

395   in the year (Figure 9b). Various transportation pathways are likely working in opposing directions to influence settlement at different locations. Average cross-shelf transport has previously indicated a break over the mid-latitudes of WA (Wijeratne et al. 2018, Figure 9).
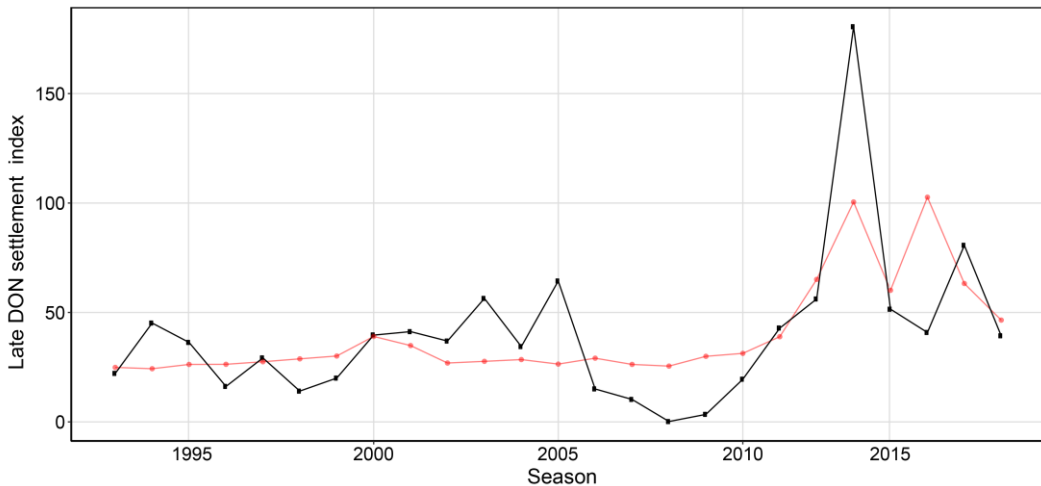
Figure 10 Observed (black) and modelled (red) late Dongara (DON) settlement index from 1993 to 2018. The red line is the most parsimonious model extended to 1993.

On an annual timescale, increased strength in KE in the northern offshore areas of the fishery (Figure 1) was associated with a decrease in puerulus settlement in the early portion of the season. It is not uncommon for the advective behaviour of large-scale eddies to negatively affect crustacean species (Medel et al., 2018; Nieto et al., 2014). Retention and dispersal of larvae can also differ in persistent eddy scenarios where a more uniform shape likely leads to retention. However, a more eccentric shape leads to dispersal (Cetina-Heredia et al., 2019b). Earlier studies suggest an increase in the number of eddies positively influence the retention of larvae and, therefore, transport across the shelf and to the nearshore (Griffin et al., 2001; Yeung et al., 2001; Cetina-Heredia et al., 2019a, 2015). This is contradictory to our results. Our study used the mean annual KE over a large spatial area, and the site in question is north of the highest density of puerulus settlement. Using a large spatial area, we have omitted the influence of sub-mesoscale features within the region, which could impact a puerulus' ability to cross the shelf and reach coastal habitats (Cosoli et al., 2020).

The GAM analyses suggest that different environmental drivers influence PI at each site, but this varies depending on when puerulus returns to shore (early or late, Figures 9a and 9b). However, we can establish discernible patterns with some certainty and physical relevance. Sites closer in latitude have similar results, Abrolhos and Cape Mentelle being the exception. Abrolhos is located off the shelf and has historically had different trends in PI compared to other locations and even on the adjacent coast. The Abrolhos PI has also recovered to pre-failure levels, whereas coastal locations have not, particularly at Lancelin and locations further south (Kolbusz et al., 2021). Cape Mentelle has historically had a low settlement and also has a unique location being the farthest south. Early settlement at Cape Mentelle also had little difference between all top models within 2 AIC of the most parsimonious model (cross-shelf transport at 33° S during spawning season). Despite one variable having the highest importance and being in the top model, there was little difference between all models within 2 AICc units.

Given the several months over which lobster larvae hatch, followed by their prolonged pelagic life cycle and settlement estimated to occur some 9-11 months later (Phillips, 1981), the large amount of variation and lack of solid

relationships between environmental or biological predictors and PI was not unexpected (Figure 2). However, we have revealed patterns up and down the coast, suggesting that both biological and environmental predictors can have a strong and sometimes consistent influence on puerulus settlement for adjacent sites.

4.3 Variation in oceanographic conditions

All the oceanographic factors examined here have been suggested to directly influence *P. cygnus* larvae at some point in their first year of life. Over time, the forcing and interactions between these environmental variables were too complex to examine in the multiple regression analysis. However, they may have as much influence on successful puerulus settlement as instantaneous values used. Furthermore, the various oceanographic mechanisms act differently, sometimes in competition (Figures 9a and b), to provide contrasting results for the different sites. Using the above multiple regression analysis results as an exploratory tool, we have additionally drawn upon patterns in the south-east Indian Ocean and WA coastal zone over the last two decades. This includes lagging conditions, alongside the fishery changes, that may have contributed to the "worst-case scenario" and resulted in the recruitment failure in 2008 - 2009.

4.3.1 Inter-annual: Hiatus period and cross-shelf transport

Over the past 30 years, links between ENSO events and the PI have been well documented using the SOI (Figure 3) (Caputi et al., 2001; Pearce and Phillips, 1988). Warmer temperatures are experienced during stronger LC conditions evident during the La Niña phase (positive SOI), providing better conditions for larval development. The SOI record since these relationships began highlights the possibility of sustained neutral ENSO conditions to be a reason for this breakdown (Pattiaratchi and Hetzel, 2020; Pattiaratchi and Siji, 2020). From 2000 until 2009, neither a moderate La Niña phase nor a moderate El Niño phase occurred, and consequently, the energy in the system also decreased (Figure 3). After 2009, an unusually strong LC (La Niña, 2011) was preceded by an unusually weak year (El Niño, 2010) (Huang and Feng, 2015). Before 2008 there were fluctuations in LC strength, or phases of moderate strength, over several seasons whilst the puerulus settlement also fluctuated similarly (Figure 3, and Caputi et al., 2001, Figure 6). An extended period (> 5 years) of low or neutral ENSO conditions, termed a hiatus, had not yet been experienced since puerulus collection began; therefore, the relationship breakdown is not surprising. Recovery in puerulus numbers began after the strong La Niña in 2011, taking a few seasons to reach levels before 2000. If these strong La Niña conditions had not occurred, what would have been the response? Whether this delayed recovery was due to the climate inertia in the system adjusting or changes in recruitment numbers after changes in the fishing the spawning stock is uncertain.
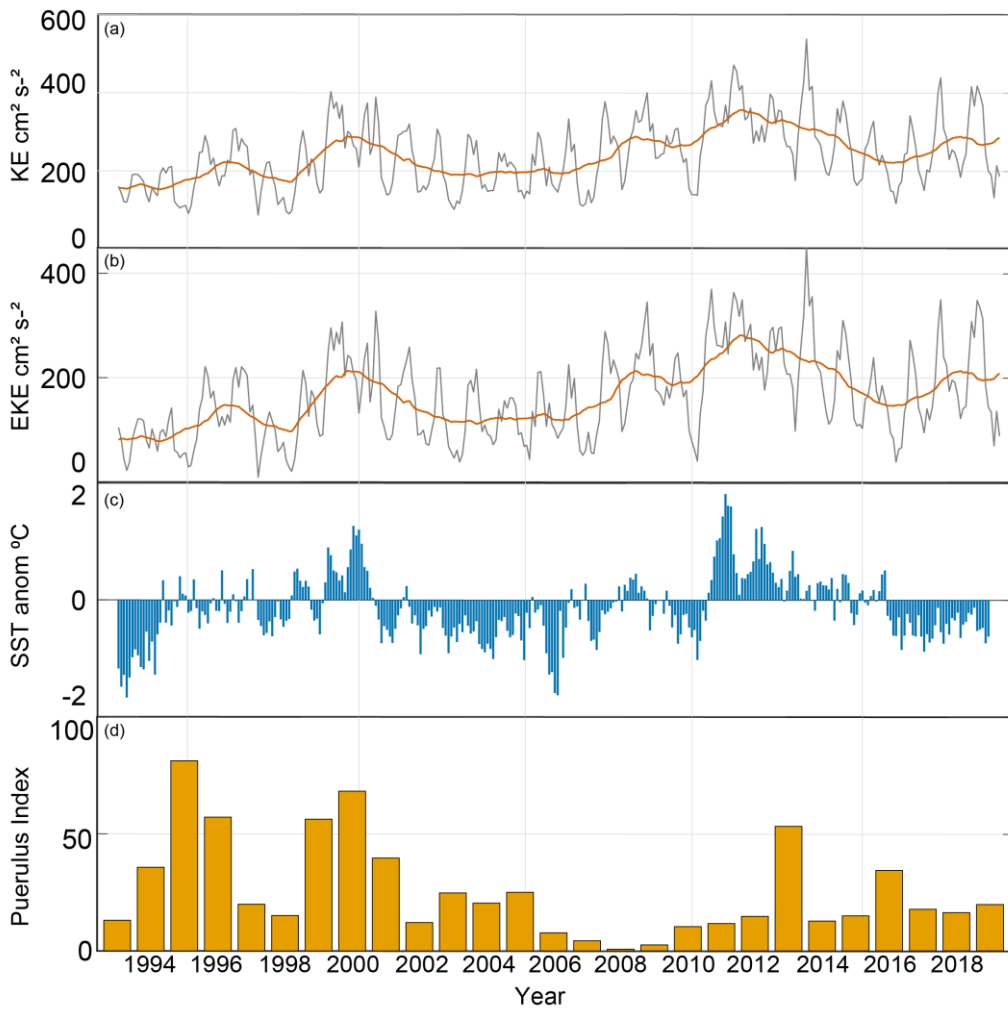
Figure 11 (a) Kinetic energy and (b) eddy kinetic energy (cm² s⁻²) from altimeter data, the (c) SST (⁰C) anomaly from SSTAARS and (d) PI for the whole Western rock lobster fishery.

Similarly, SST anomalies (Figure 11) have periods of neutral conditions and below-average temperatures, respectively, from approximately 2000 to 2008 (Pattiaratchi and Hetzel, 2020). These extended low activity conditions may have caused a shift in the conditions experienced by pelagic western rock lobster larvae. The patterns may be due to atmospheric and oceanic processes that imprint themselves upon the SST field. The ocean's thermal energy is transferred to the atmosphere via the sea surface, which the SST controls. Thus, SST on a spatial scale plays a crucial role in regulating climate and variability. The extended period of cooler SST anomalies may have contributed to the low 2008 and 2009 settlements. A decreasing PI over the start of the century was in line with these patterns. Then recovery followed the maxima experiences with the 2011/12 La Niña (Boening et al., 2012), which perhaps took the system some years to return to conditions as usual. Thus, it may not be a season-specific factor that has caused the years of low settlement in the late 2000s. Instead,

consecutive years of these 'hiatus' conditions (Figure 11) have driven a regime shift in the environment impacting *P. cygnus* pelagic life stages (DeYoung et al., 2004).
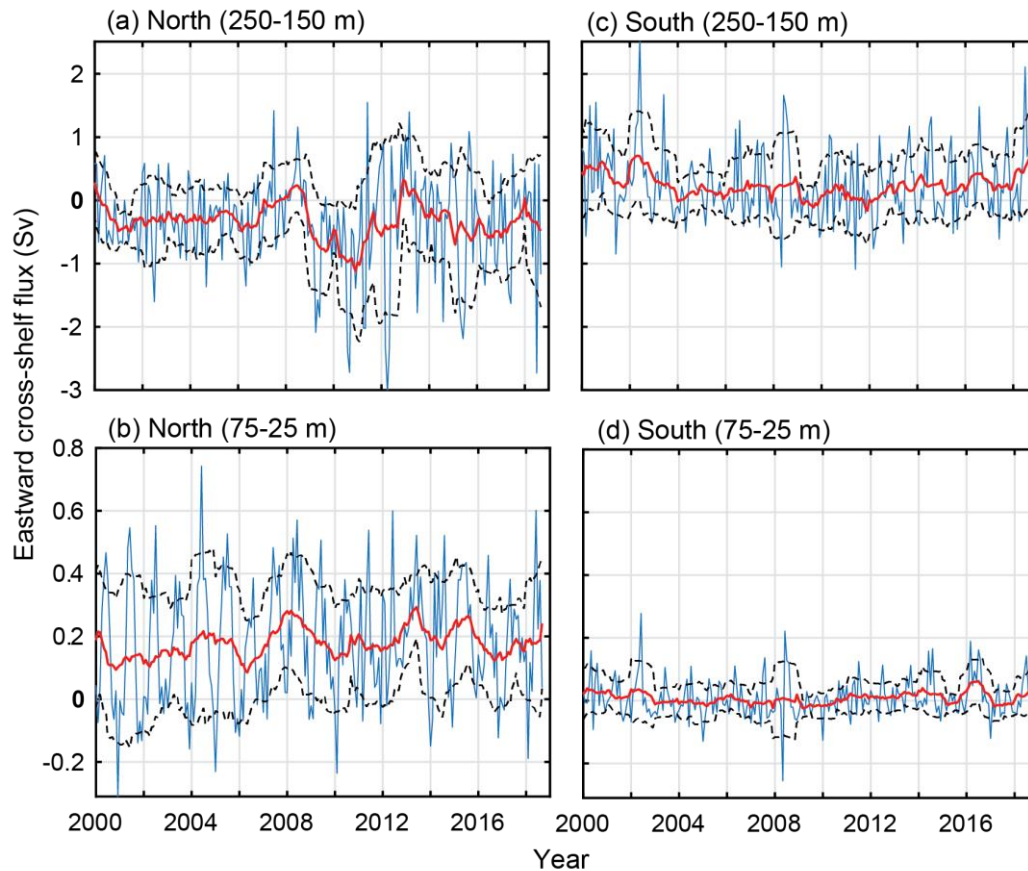
Figure 12 Cross-shelf transport (easterly) between 2000 and 2018 off the shelf. North and south divide are shown in Figure 1a. (a) North cross-shelf flux between 250-150 m and (b) 75-25 m. (c) South cross-shelf flux between 250-150 m and (d) 75-25 m. The yearly moving mean (red) and the positive and negative moving standard deviation (dashed black) are included.

Despite cross-shelf transport being a forcing mechanism behind larval transport into the nearshore, a lack of statistical relationships was found through the multiple regression analysis. Given the 'hiatus' conditions or shift after 2008 in the LC, one would expect some form of accompanying change in cross-shelf flux (Pattiaratchi and Hetzel, 2020). Over the 50 metre contour, there are no noticeable inter-annual changes over the 18 years between the south or north boxes. In the south, there is minor variation in the standard deviation from the mean (Figure 12, dashed lines); however, it is predominantly onshore transport on the shelf (50 m) and over the continental shelf (200 m). The cross-shelf transport in the north shows an apparent increase in variability over the continental shelf (Figure 12, 200 m) after 2008, highlighting the increased movement in water over the northern part of the fishery (Figure 12). This is also where the LC increases over the summer (Figure 5b) and puerulus settlement shifts.

4.3.1 Seasonal: Capes Current and Leeuwin Current interactions during summer

Before 2008, conditions were reasonably neutral over the early settlement season, leading to high/low puerulus settlement potentially controlled by oceanographic and biological factors (Figure 13). Since 2009, the LC dominates (blue years skewed to the right, Figure 13), possibly causing average to low puerulus conditions across all sites. Except for Cape Mentelle, the southern-most site and potentially most isolated from the LC (Figure 14h). Comparatively, over the late period of settlement (Figure 14), the CC dominates the system, with higher settlement occurring later in the summer. Thus, the years of recruitment failure have neutral conditions where neither the CC nor LC is particularly dominant over the latter portion of the season. The same exists for 2007 and 2008 during the early portion of the season. Interestingly, during these recruitment failure years, the spatial extent of the LC during spring months was more considerable or on par with the six months prior, when newly hatched phyllosoma transport across the shelf into the open ocean may have also been impacted (Huang and Feng, 2015).

These patterns suggest that perhaps a timing mismatch is in play, suggested previously by de Lestang et al. (de Lestang et al., 2015). While puerulus are crossing the shelf, an increase in LC strength may transport them past Cape Mentelle, away from suitable habitats. In contrast, a strong CC is likely to assist transport northward along the shelf, increasing settlement over the later season. Interaction between these two critical currents over the shelf influences the movement of puerulus onshore and needs to be investigated in greater detail. Particle tracking modelling over these months would be a possible way to investigate these interactions; however, this is beyond the scope of the present study.
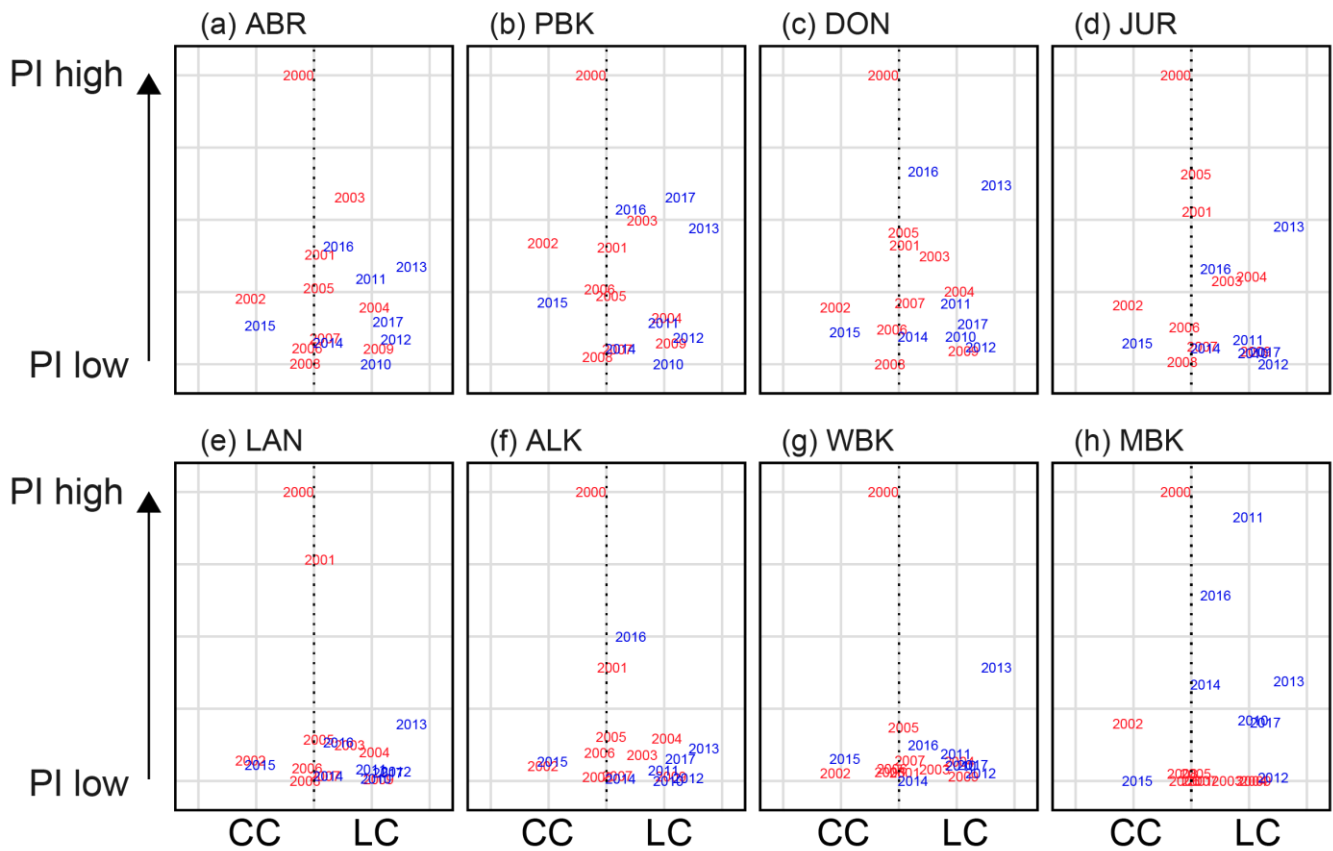
495 **Figure 13 Relationship of the more dominant current during the early spring/early summer (September - November) to early PI at monitoring sites (a) Abrolhos (b) Port Gregory (c) Dongara (d) Jurien Bay (e) Lancelin (f) Alkimos (g) Warnbro and (h) Cape Mentelle. The x-axis is the difference between the LC and CC standardized, providing an indication of which is more prominent at the time. Red indicates the seasons before the recruitment failure, blue indicates seasons after.**
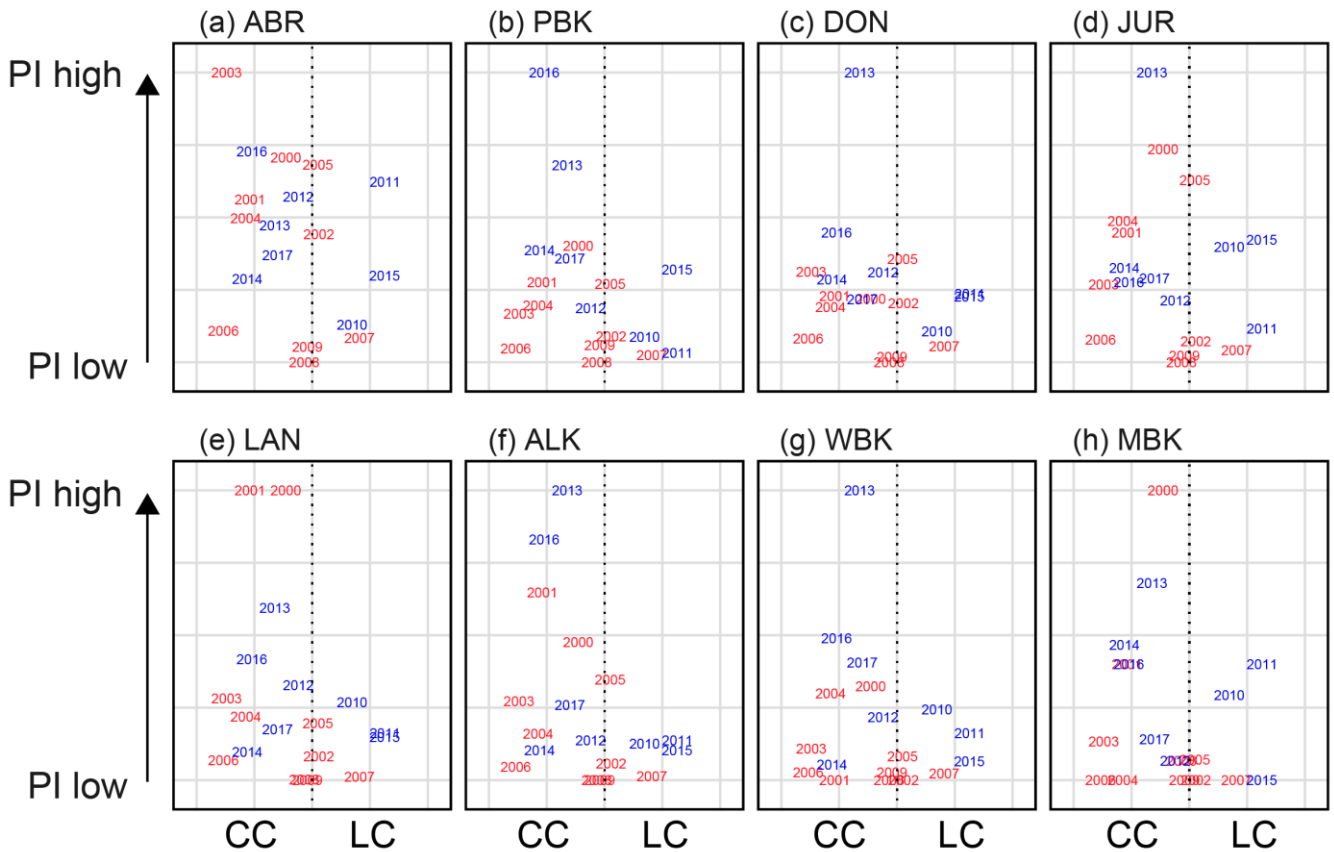
500 **Figure 14 Relationship of the more dominant current during the late summer/early autumn (December - March) to late PI at monitoring sites (a) Abrolhos (b) Port Gregory (c) Dongara (d) Jurien Bay (e) Lancelin (f) Alkimos (g) Warnbro and (h) Cape Mentelle. The x-axis is the difference between the LC and CC standardized, indicating which is more prominent at the time. Red indicates the seasons before the recruitment failure; blue indicates seasons after.**

5 Conclusions and Implications

505   The objective of the current study was to determine oceanographic and biological factors that may explain the previously

unexplained failure of puerulus settlement (2008-2009) and subsequent change in the proportions of puerulus settling in early

vs late parts of the season (Kolbusz et al., 2021). The study was completed through an exploratory multiple regression analysis

encompassing direct oceanographic and biological factors likely to influence the pelagic early-life cycle of *P. cygnus*. The

main conclusions were as follows:

510   ● Local oceanographic and biological conditions greatly influence *P. cygnus*, as settlement of puerulus at adjacent sites

        along the coast tend to be influenced by similar oceanographic and biological variables. Offshore, the Abrolhos

        Islands had a unique yet consistent pattern of settlement that correlated with particular oceanographic and biological

        factors.

- On a fishery-wide scale, the period of recruitment failure (2008 and 2009) and the associated low settlement period (2004 – 2010) coincided with a hiatus period in the Leeuwin Current system. This was associated with mainly neutral ENSO conditions and slightly cooler SST anomalies.

- Increased KE in the northern region of the fishery was negatively correlated to puerulus settlement in the early period of the season, whilst the KE (and EKE) in the southern region was positively correlated at selected sites. This suggests different driving mechanisms over the whole range of latitudes that encompass the fishery for settlement early and later in the season.

- Seasonal variation of the LC system likely controls the conditions that favour increased puerulus settlement. During the summer months of hatching, a strong LC negatively affects puerulus settlement at central sites after their pelagic phase. During the subsequent winter, the system is dominated by a strong southward LC and its associated eddies, which then assists onshore phyllosoma transport. Then, whilst the newly metamorphosed puerulus are moving onshore across the LC, should it be too strong, the current can negatively impact settlement at the northern sites but positively impact the southern sites.

- An increase in the strength of the LC in the summer months since 2006, combined with a decrease in the strength of the CC over the early summer months, may have caused a timing mismatch for puerulus settling on nearshore reefs. If the LC were stronger in summer, a strong CC would be needed to counteract the southward flow to get the puerulus transported northward, which has occurred in recent years. However, the CC in the latter half of the summer has been less variable and has not declined to the same extent, potentially explaining the trend of better settlement later in the season.

- Between 2008 and 2011, the cross-shelf transport in the northern half of the fishery across the continental shelf became more variable whilst consistently offshore. This overlap with the period of recruitment failure suggests that cross-shelf transport in an offshore direction could have reduced the transport and subsequent settlement of puerulus onshore.

These findings have implications for fisheries management and their modelling of future stocks of catchable western rock lobsters. Environmental conditions are suspected of altering the puerulus settlement, which can be incorporated in planning and management. For example, reductions in the fishing effort can encourage an increase in larvae for the following season (de Lestang et al., 2015).

Despite its exploratory nature, this study offers insight into factors potentially behind the recruitment failure that have not been addressed before. It also expands our current understanding of what oceanographic variables potentially influence puerulus settlement and how the variables themselves are intertwined in this complex system. With the available numerical modelled data, we can show that it is not solely the LC that is the dominating factor behind puerulus settlement variability but the CC, cross-shelf flow, and the system's state as a whole.

Appendix A

Table A1. Oceanographic data sources and sites used to calculate the 40 predictor variables included in time series analysis. Unless stated, the timing is within the season of puerulus settlement. Spawning season indicates that the variable is from the year prior or within the spawning season as larvae hatch.

Predictor Variable	Data source	Northern	Central		Southern	No. Variables
Leeuwin Current strength (Austral winter mean)	ozROMS	27ºS	30ºS		34º S	3
Leeuwin Current strength (Austral summer mean) Spawning season	ozROMS	27ºS	30ºS		34º S	3
Leeuwin Current strength (Austral summer mean)	ozROMS	27ºS	30ºS		34º S	3
Capes Current strength (Austral spring mean)	ozROMS	27ºS	30ºS		34ºS	3
Capes Current strength (Austral summer mean)	ozROMS	27ºS	30ºS		34ºS	3
Capes Current strength (Austral spring mean) Spawning season	ozROMS	27ºS	30ºS		34ºS	3
Capes Current strength (Austral summer mean) Spawning season	ozROMS	27ºS	30ºS		34ºS	3
Cross-shelf transport – offshore (spawning season) 150 – 50 m (September - March mean)	ozROMS	26-28ºS 28-30ºS	30-32º S 33-33ºS			4
Cross-shelf transport – onshore 150 – 50 m (April - September mean)	ozROMS	26-28ºS 28-30ºS	30-32º S 33-33ºS			4
Bottom temperature (October - March) Spawning season	ozROMS	24.5-30.5°S		30.5-34.5°S		2
EKE (January – December mean)	ozROMS	24.5-30.5°S		30.5-34.5°S		2
KE (January – December mean)	ozROMS	24.5 - 30.5°S		30.5-34.5°S		2
SST October – March mean (summer) April - September mean (winter)	SSTARS, Integrated Marine Observing System (IMOS, oceancurrent.imos.org.au) Australian Ocean Data Network (AODN) portal (portal.aodn.org.au) (Wijffels et al. 2018)	WA waters extent 21ºS-36ºS 108ºE to coastline				2
Temperature in the top 100 m	ozROMS	WA waters extent 21ºS-36ºS				1

(January – December mean)		108ºE to coastline			
Independent Breading Stock Survey (IBSS) Spawning season	DPIRD	Index for whole fishery			1
			Total predictor variables		39

Appendix B

Table B1. Top generalised additive models (GAMs) for predicting the early puerulus settlement at the eight sites from full subset analyses. Difference between lowest reported corrected Akaike Information Criterion (ΔAICc), AICc weight (ωAICc), variance explained (R^2) and effective degrees of freedom (EDF) are reported for model comparison. Model selection was based on the most parsimonious model (fewest variables) within two units of the lowest AICc, and models are ordered by parsimony.

Site	Model	ΔAICc	ωAICc	R^2	EDF
Abrolhos	KE North	0	0.032	0.30511	2
	CC 27° S early + KE North	1.98	0.012	0.33571	3
Port Gregory	CC 30° S early (spawning season) + KE North + LC 27 °S winter	0	0.06	0.64656	4
	KE north +LC 27°S winter	0.668	0.043	0.56042	3
Dongara	CC 27° S early	0	0.017	0.24911	2
	KE north	0.584	0.012	0.24508	2
	CC 27° S early + KE north	0.933	0.01	0.34984	3
	KE north + LC 27º S winter	1.523	0.008	0.43133	3
	KE north + Xshore 29 º S (spawning season)	1.677	0.007	0.42171	3
	CC 27° S early + Xshore 27º S	1.843	0.007	0.30153	3
	CC 27° S early + LC 27º S winter	1.939	0.006	0.35149	3
Jurien Bay	CC 27° S early + LC 27º S (spawning season)	0	0.018	0.37311	3
	CC 27º S early + CC 27º S late (spawning season)+KE north	0.071	0.017	0.41751	4
	CC 27°S early + LC 30º S (spawning season)	0.373	0.015	0.36202	3
	KE north + Xshore 31º S	0.408	0.015	0.41185	3
	KE north + LC 30º S (spawning season) + Xshore 29º S (spawning season)	0.877	0.012	0.52731	4
	KE South + LC 30º S (spawning season) + Xshore 29º S (spawning season)	1.186	0.01	0.59535	4
	CC 27º S early +KE north+ LC 30º S (spawning season)	1.322	0.009	0.52225	4
	EKE south + LC 30º S (spawning season)+ Xshore 29º S (spawning season)	1.446	0.009	0.58966	4
	CC 27°S early	1.735	0.008	0.1932	2
	EKE south + KE north+ Xshore 31º S	1.755	0.008	0.53007	4
	KE north + LC 27º S (spawning season)	1.782	0.007	0.40766	3
	KE north + LC 30º S (spawning season) + Xshore 31º S (spawning season)	1.839	0.007	0.50423	4
	CC 27º S early +KE north + LC 27º S (spawning season)	1.895	0.007	0.49805	4
Lancelin	KE north+ KE South +LC 27º S (spawning season)	0	0.044	0.66194	4

KE south+ LC 30º S (spawning season) + Xshore 27º S (spawning season)	0.977	0.027	0.54491	4
EKE south + KE north+ Xshore 31º S	1.26	0.023	0.5726	4
KE north + KE South+ Xshore 31º S	1.483	0.021	0.57312	4
KE south + LC 27º S (spawning season)	1.711	0.019	0.68503	3
KE north + KE south	1.911	0.017	0.53142	3
EKE south + KE north + LC 27º S (spawning season)	1.953	0.017	0.60116	4

Location	Model			
Alkimos	KE north + KE South+ SST Winter	0	0.02	0.68482	4
	KE south + SST Winter	0.084	0.019	0.59854	3
	CC 27 º S early + KE South + SST Winter	0.608	0.015	0.63389	4
	KE north	0.633	0.015	0.29904	2
	EKE South + KE north + SST Winter	0.91	0.013	0.6593	4
	EKE South + SST Winter	0.966	0.012	0.58518	3
	KE South + SST Winter + Xshore 27 º S (spawning season)	1.214	0.011	0.67061	4
	KE South + SST Summer + Xshore 31º S (spawning season)	1.392	0.01	0.57343	4
	CC 27 º S early + EKE South + SST Winter	1.509	0.009	0.62109	4
	EKE North + KE South + SST Winter	1.535	0.009	0.66072	4
	KE north + KE South	1.838	0.008	0.48649	3
	EKE south + KE North	1.864	0.008	0.48183	3
	CC 27 º S early + KE South + SST Summer	1.92	0.008	0.55349	4
	KE north+ SST Winter	1.967	0.008	0.36099	3
Warnbro	Xshore 27º S + Xshore 31º S (spawning season)	0	0.01	0.63867	3
	LC 27º S winter	0.788	0.006	0.31409	2
	Xshore 27º S	1.115	0.005	0.34867	2
	CC 27º S early +LC 27º S winter	1.165	0.005	0.50841	3
	Xshore 29º S (spawning season)	1.166	0.005	0.26977	2
	Xshore 31º S (spawning season)	1.436	0.005	0.27396	2
	CC 30º S early (spawning season) + Xshore 27º S	1.579	0.004	0.47095	3
	LC 30º S (spawning season) + Xshore 31º S (spawning season)	1.62	0.004	0.37919	3
	CC 27º S early	1.699	0.004	0.28026	2
	IBSS+ Xshore 31º S	1.701	0.004	0.50221	3
	CC 27º S early + Xshore 29º S	1.706	0.004	0.46989	3
	CC 27º S early + Xshore 31º S	1.719	0.004	0.44596	3
	LC 30º S (spawning season) + Xshore 27º S + Xshore 31º S (spawning season)	1.758	0.004	0.6657	4
	LC 27º S winter + Xshore 31º S	1.795	0.004	0.43706	3
	CC 27º S early + Xshore 29º S (spawning season)	1.805	0.004	0.4228	3
	Xshore 27º S + Xshore 29º S (spawning season)	1.986	0.004	0.50025	3
Cape Mentelle	Xshore 33º S (spawning season)	0	0.008	0.33639	2
	LC 27º S	0.008	0.008	0.39289	2
	Xshore 31º S (spawning season)	0.408	0.006	0.31403	2
	CC 30º S late (spawning season)	0.484	0.006	0.27898	2
	SST summer	0.484	0.006	0.34543	2

	ΔAICc	ωAICc	R²	EDF
CC 27º S early (spawning season)	0.676	0.006	0.20266	2
LC 30º S (spawning season)	0.8	0.005	0.20202	2
CC 34º S early (spawning season)	0.945	0.005	0.16214	2
CC 34º S late (spawning season)	1.008	0.005	0.20141	2
Bottom temperature	1.222	0.004	0.14284	2
CC 27º S late (spawning season)	1.262	0.004	0.16047	2
CC 27º S early	1.27	0.004	0.15818	2
EKE north	1.37	0.004	0.13383	2
Top 100m temp	1.446	0.004	0.12044	2
LC 34º S (spawning season)	1.528	0.004	0.10325	2
Xshore 33º S	1.533	0.004	0.09786	2
SST Winter	1.545	0.004	0.10168	2
IBSS	1.583	0.004	0.09485	2
CC 34º S early	1.702	0.003	0.05667	2
Xshore 31º S	1.806	0.003	0.04445	2
KE south	1.808	0.003	0.05125	2
Xshore 27º S (spawning season)	1.858	0.003	0.03529	2
EKE south	1.879	0.003	0.03523	2
Xshore 29º S (spawning season)	1.933	0.003	0.02133	2
Xshore 27º S	1.979	0.003	0.01187	2
KE north	1.979	0.003	0.01289	2

Table B2. Top generalised additive models (GAMs) for predicting the late puerulus settlement at the eight sites from full subset analyses. Difference between lowest reported corrected Akaike Information Criterion (ΔAICc), AICc weight (ωAICc), variance explained (R^2) and effective degrees of freedom (EDF) are reported for model comparison. Model selection was based on the most parsimonious model (fewest variables) within two units of the lowest AICc, and models are ordered by parsimony.

Site	Model	ΔAICc	ωAICc	R^2	EDF
Abrolhos	KE North	0	0.009	0.21872	2
	LC 27° S summer	0.456	0.007	0.1768	2
	KE North + LC 30° S winter	1.711	0.004	0.28972	3
	CC 30° S late (spawning season) + LC 27°S summer	1.904	0.003	0.30444	3
Port Gregory	IBSS + LC 30° S summer + Xshore 31º S	0	0.103	0.70071	4
	IBSS + LC 30° S (spawning season) + LC 30° S summer	1.151	0.058	0.57984	4
	IBSS + LC 30° S summer	1.639	0.046	0.62492	3
Dongara	IBSS + LC 30° S (spawning season)	0	0.021	0.45068	3
	IBSS	0.808	0.014	0.4202	2
	IBSS + KE North	1.984	0.008	0.48773	3
Jurien Bay	IBSS + LC 30° S (spawning season)	0	0.056	0.51808	3
	EKE north + IBSS + LC 30° S (spawning season)	1.301	0.029	0.58445	4
	CC 27º S early + IBSS + LC 30° S (spawning season)	1.702	0.024	0.55792	4
Lancelin	KE south	0	0.013	0.55565	2
	EKE south	0.599	0.01	0.51543	2
	Top 100m Temp	1.922	0.005	0.31946	2

	KE south+ Xshore 27º S (spawning season)	1.953	0.005	0.55691	3
	EKE south + IBSS	1.96	0.005	0.47425	3
Alkimos	KE south + LC 27° S winter	0	0.021	0.53502	3
	EKE south + LC 27° S winter	0.01	0.02	0.50903	3
	CC 30º S late + EKE south + LC 27°S winter	1.852	0.008	0.60733	4
Warnbro	CC 34º S early + LC 27º S winter	0	0.019	0.47117	3
	CC 34º S early + Xshore 27º S (spawning season)	1.153	0.01	0.39126	3
	CC 34º S early + LC 27º S winter + LC 34º S summer	1.612	0.008	0.44042	4
	LC 27º S winter	1.705	0.008	0.42669	2
	CC 34º S early + IBSS	1.877	0.007	0.41882	3
	CC 30º S late (spawning season) + LC 27°S winter	1.973	0.007	0.61929	3
Cape Mentelle	Xshore 33º S (spawning season)	0	0.014	0.48806	2

Data Availability

The dataset for this research and relevant contacts can be found through the Department of Primary Industries and Regional Development website. http://www.fish.wa.gov.au/Species/Rock-Lobster/Lobster-Management/Pages/Puerulus-Settlement-Index.aspx

The ozROMS numerical model outputs are available at this THREDDS server http://130.95.29.56:8080/thredds/catalog.html

Author contribution

JK completed the analysis of the data and conclusions under the guidance of CH, TL, and SdL. JK wrote the manuscript and produced the figures with the help and inputs from all co-authors. TL developed the code for the multiple regression analysis (Fisher et al. 2016). All authors contributed to the article and approved the submitted version.

Competing interests

The authors declare that they have no conflict of interest

Acknowledgements

We would like to acknowledge the Department for Primary Industries and Regional Development (Fisheries) for the use of raw puerulus collector data. Thank you to Rebecca Fisher for her assistance with the multiple regression analysis toolbox. Thank you to Sarath Wijeratne for ozROMS data processing assistance.

References

Akaike, H.: Information theory and an extension of the maximum likelihood principle, Second Int. Symp. Inf. Theory, 267–281, 1973.

585 Andrews, J. C.: Eddy structure and the West Australian current, Deep. Res., 24, 1133–1148, https://doi.org/10.1016/0146-6291(77)90517-3, 1977.

Batteen, M. L., Kennedy, R. A., and Miller, H. A.: A process-oriented numerical study of currents, eddies and meanders in the Leeuwin Current System, Deep. Res. Part II Top. Stud. Oceanogr., 54, 859–883, https://doi.org/10.1016/j.dsr2.2006.09.006, 2007.

590 Benthuysen, J., Feng, M., and Zhong, L.: Spatial patterns of warming off Western Australia during the 2011 Ningaloo Niño: Quantifying impacts of remote and local forcing, Cont. Shelf Res., 91, 232–246, https://doi.org/10.1016/j.csr.2014.09.014, 2014.

Berthot, A., Pattiaratchi, C., Feng, M., Meyers, G., and Li, Y.: Understanding the natural variability of currents along the Western Australian coastline, The SRFME initiative and the SRFME collaborative linkages program, 2007.

595 Boening, C., Willis, J. K., Landerer, F. W., Nerem, R. S., and Fasullo, J.: The 2011 La Niña : So strong , the oceans fell, Geophys. Res. Lett., 39, 1–5, https://doi.org/10.1029/2012GL053055, 2012.

Bureau of Meteorology: Fremantle Mean Sea Level, 2021a.

Bureau of Meteorology: Southern Oscillation Index, 2021b.

Burnham, K. and Anderson, D.: Model Selection and Multimodel Inference, Springer New York, 2002.

600 Caballero, A., Pascual, A., Gerald, D., and Infantes, M.: Sea Level and Eddy Kinetic Energy variability in the Bay of Biscay inferred from satellite altimeter data, J. Mar. Syst., 72, 116–134, https://doi.org/10.1016/j.jmarsys.2007.03.011, 2008.

Caputi, N.: Impact of the Leeuwin Current on the spatial distribution of the puerulus settlement of the western rock lobster (Panulirus cygnus) and implications for the fishery of Western Australia, Fish. Oceanogr., 17, 147–152, https://doi.org/10.1111/j.1365-2419.2008.00471.x, 2008.

605 Caputi, N. and Brown, R.: The effect of environment on puerulus settlement of the western rock lobster (Panulirus cygnus) in Western Australia, Fish. Oceanogr., 2, 1–10, https://doi.org/10.1111/j.1365-2419.1993.tb00007.x, 1993.

Caputi, N., Chubb, C., and Brown, R.: Relationships between Spawning Stock, Environment, Recruitment and Fishing Effort for the Western Rock Lobster, Panulirus Cygnus, Fishery in Western Australia, 68, 213–226, https://doi.org/10.1163/156854095X00115, 1995.

610 Caputi, N., Chubb, C., and Pearce, A.: Environmental effects on recruitment of the western rock lobster, Panulirus cygnus, Mar. Freshw. Res., 52, 1167–1174, https://doi.org/10.1071/MF01180, 2001.

Caputi, N., Melville-Smith, R., de Lestang, S., Pearce, A., and Feng, M.: The effect of climate change on the western rock lobster (Panulirus cygnus) fishery of Western Australia, Can. J. Fish. Aquat. Sci., 67, 85–96, https://doi.org/10.1139/F09-167, 2010.

615 Caputi, N., Feng, M., de Lestang, S., Denham, A., Penn, J., Slawinski, D., Pearce, A., Weller, E., and How, J.: Identifying factors affecting the low western rock lobster puerulus settlement in recent years, https://doi.org/na, 2014.

Caputi, N., Chandrapavan, A., Kangas, M., de Lestang, S., Hart, A., Johnston, D., and Penn, J.: Stock-recruitment-environment relationships of invertebrate resources in Western Australia and their link to pro-active management harvest strategies, Mar. Policy, 133, 1–16, https://doi.org/10.1016/j.marpol.2021.104728, 2021.

620 Cetina-Heredia, P., Roughan, M., van Sebille, E., Feng, M., and Coleman, M.: Strengthened currents override the effect of warming on lobster larval dispersal and survival, Glob. Chang. Biol., 21, 4377–4386, https://doi.org/10.1111/gcb.13063, 2015.

Cetina-Heredia, P., Roughan, M., Liggins, G., Coleman, M., and Jeffs, A.: Mesoscale circulation determines broad spatio-temporal settlement patterns of lobster, PLoS One, 14, 1–20, https://doi.org/10.1371/journal.pone.0211722, 2019a.

Cetina-Heredia, P., Roughan, M., van Sebille, E., Keating, S., and Brassington, G.: Retention and Leakage of Water by
625 Mesoscale Eddies in the East Australian Current System, J. Geophys. Res. Ocean., 124, 2485–2500, https://doi.org/10.1029/2018JC014482, 2019b.

Chittleborough, R.: Environmental factors affecting growth and survival of juvenile western rock lobsters *Panulirus longipes* (Milne-Edwards), Mar. Freshw. Res., 26, 177–196, https://doi.org/http://dx.doi.org/10.1071/MF9750177, 1975.

Chittleborough, R.: Growth of Juvenile Panulirus Longipes Cygnus George on Coastal Reefs Compared with those Reared
630 Under Optimal Environmental Conditions, Mar. Freshw. Res., 27, 279–295, https://doi.org/10.1071/MF9760279, 1976.

Chubb, C.: No Measurement of spawning stock levels for the western rock lobster Panulirus cygnus, Rev. Investig. Mar., 12, 223–233, 1991.

Clarke, A. and Li, J.: El Niño/La Niña shelf edge flow and Australian western rock lobsters, Geophys. Res. Lett., 31, https://doi.org/10.1029/2003GL018900, 2004.

635 Cosoli, S., Pattiaratchi, C., and Hetzel, Y.: High-frequency radar observations of surface circulation features along the south-western australian coast, J. Mar. Sci. Eng., 8, https://doi.org/10.3390/jmse8020097, 2020.

Cresswell, G., Boland, F., Peterson, J., and Wells, G.: Continental shelf currents near the Abrolhos Islands, Western Australia, Mar. Freshw. Res., 40, 113–128, https://doi.org/10.1071/MF9890113, 1989.

DeYoung, B., Harris, R., Alheit, J., Beaugrand, G., Mantua, N., and Shannon, L.: Detecting regime shifts in the ocean: Data
640 considerations, Prog. Oceanogr., 60, 143–164, https://doi.org/10.1016/j.pocean.2004.02.017, 2004.

Ehrhardt, N. and Fitchett, M.: Dependence of recruitment on parent stock of the spiny lobster, *Panulirus argus*, in Florida, Fish. Oceanogr., 19, 434–447, https://doi.org/10.1111/j.1365-2419.2010.00555.x, 2010.

Fang, F. and Morrow, R.: Evolution, movement and decay of warm-core Leeuwin Current eddies, Deep. Res. Part II Top. Stud. Oceanogr., 50, 2245–2261, https://doi.org/10.1016/S0967-0645(03)00055-9, 2003.

645 Feng, M., Meyers, G., Pearce, A., and Wijffels, S.: Annual and interannual variations of the Leeuwin Current at 32 ° S, J. Geophys. Res., 108, 19–39, https://doi.org/10.1029/2002JC001763, 2003.

Feng, M., Wijffels, S., Godfrey, S., and Meyers, G.: Do eddies play a role in the momentum balance of the Leeuwin Current?, J. Phys. Oceanogr., 35, 964–975, https://doi.org/10.1175/JPO2730.1, 2005.

Feng, M., Slawinski, D., Beckley, L., and Keesing, J.: Retention and dispersal of shelf waters influenced by interactions of

650   ocean boundary current and coastal geography, Mar. Freshw. Res., 61, 1259–1267, https://doi.org/10.1071/MF09275, 2010.

Feng, M., Caputi, N., Penn, J., Slawinski, D., de Lestang, S., Weller, E., and Pearce, A.: Ocean circulation, stokes drift, and connectivity of western rock lobster (*Panulirus cygnus*) population, Can. J. Fish. Aquat. Sci., 68, 1182–1196, https://doi.org/10.1139/f2011-065, 2011.

Fisher, R., Wilson, S., Sin, T., Lee, A., and Langlois, T.: A simple function for full-subsets multiple regression in ecology with

655   R, Ecol. Evol., 8, 6104–6113, https://doi.org/10.1002/ece3.4134, 2018.

Gersbach, G., Pattiaratchi, C., Ivey, G., and Cresswell, G.: Upwelling on the south-west coast of Australia - Source of the Capes Current, Cont. Shelf Res., 19, 363–400, https://doi.org/10.1016/S0278-4343(98)00088-0, 1999.

Graham, M. H.: Statistical Confronting Multicollinearity in Ecological, Source Ecol. Ecol., 84, 2809–2815, https://doi.org/10.1890/02-3114, 2009.

660   Griffin, D., Wilkin, J., Chubb, C., Pearce, A., and Caputi, N.: Ocean currents and the larval phase of Australian western rock lobster, *Panulirus cygnus*, Mar. Freshw. Res., 52, 1187–1199, https://doi.org/10.1071/MF01181, 2001.

Guan, L., Chen, Y., Wilson, J., Waring, T., Kerr, L., and Shan, X.: The influence of spatially variable and connected recruitment on complex stock dynamics and its ecological and management implications, Can. J. Fish. Aquat. Sci., 76, 937–949, https://doi.org/10.1139/cjfas-2018-0151, 2019.

665   Hamon, B. .: Geostrophic currents in the southeastern Indian Ocean, Aust. J. Mar. Freshw. Res., 16, 255–271, 1965.

Hood, R., Beckley, L., and Wiggert, J.: Biogeochemical and ecological impacts of boundary currents in the Indian Ocean, Prog. Oceanogr., 156, 290–325, https://doi.org/10.1016/j.pocean.2017.04.011, 2017.

Huang, Z. and Feng, M.: Remotely sensed spatial and temporal variability of the Leeuwin Current using MODIS data, Remote Sens. Environ., 166, 214–232, https://doi.org/10.1016/J.RSE.2015.05.028, 2015.

670   Hurvich, C. and Tsai, C.: Biometrika Trust Regression and Time Series Model Selection in Small Samples, Biometrika, 76, 297–307, 1989.

Kolbusz, J., de Lestang, S., Langlois, T., and Pattiaratchi, C.: Changes in Panulirus cygnus settlement along Western Australia using a long time series, Front. Mar. Sci., 8, https://doi.org/10.3389/fmars.2021.628912, 2021.

Koslow, J., Pesant, S., Feng, M., Pearce, A., Fearns, P., Moore, T., Matear, R., and Waite, A.: The effect of the Leeuwin

675   Current on phytoplankton biomass and production off Southwestern Australia, J. Geophys. Res. Ocean., 113, 1–19, https://doi.org/10.1029/2007JC004102, 2008.

Lenanton, R., Joll, L., Penn, J., and Jones, K.: The influence of the Leeuwin Current on coastal fisheries of Western Australia, J. R. Soc. West. Aust., 74, 101–114, 1991.

de Lestang, S., Caputi, N., How, J., Melville-Smith, R., Thomson, A., and Stephenson, P.: Stock assessment for the west coast

680   rock lobster fishery, Fisheries Research Report No. 217, 1–200 pp., 2012.

de Lestang, S., Caputi, N., Feng, M., Denham, A., Penn, J., Slawinski, D., Pearce, A., and How, J.: What caused seven consecutive years of low puerulus settlement in the western rock lobster fishery of Western Australia?, ICES J. Mar. Sci., 72,

49–58, https://doi.org/10.1093/icesjms/fst048, 2015.

de Lestang, S., Caputi, N., and How, J.: Resource Assessment Report: Western Rock Lobster Resource of Western Australia,
685   Western Australian Marine Stewardship Council Report Series No. 9, Western Australian Marine Stewardship Council Report
Series, 1–139 pp., 2016.

de Lestang, S., Rossbach, M., and Blay, N.: West Coast Rock Lobster Resource Status Report 2017. In: Status Reports of the
Fisheries and Aquatic Resources of Western Australia 2016/17: The State of the Fisheries, 2018.

Luo, H., Bracco, A., and Di Lorenzo, E.: The interannual variability of the surface eddy kinetic energy in the Labrador Sea,
690   Prog. Oceanogr., 91, 295–311, https://doi.org/10.1016/j.pocean.2011.01.006, 2011.

MATLAB: Matlab R2019b, Natick, Massachusetts: The MathWorks Inc., 2019.

Medel, C., Parada, C., Morales, C., Pizarro, O., Ernst, B., and Conejero, C.: How biophysical interactions associated with sub-
and mesoscale structures and migration behavior affect planktonic larvae of the spiny lobster in the Juan Fernández Ridge: A
modeling approach, Prog. Oceanogr., 162, 98–119, https://doi.org/10.1016/j.pocean.2018.02.017, 2018.

695   Menezes, V., Phillips, H., Schiller, A., Bindoff, N., Domingues, C., and Vianna, M.: South Indian Countercurrent and
associated fronts, J. Geophsical Res. Ocean., 119, 6763–6791, https://doi.org/doi:10.1002/2014JC010076, 2014.

Meuleners, M., Ivey, G., and Pattiaratchi, C.: A numerical study of the eddying characteristics of the Leeuwin Current System,
Deep. Res. Part I Oceanogr. Res. Pap., 55, 261–276, https://doi.org/10.1016/j.dsr.2007.12.004, 2008.

Nieto, K., McClatchie, S., Weber, E., and Lennert-Cody, C.: Effect of mesoscale eddies and streamers on sardine spawning
700   habitat and recruitment success off Southern and central California, J. Geophys. Res. Ocean., 119, 6330–6339,
https://doi.org/10.1002/2014JC010251, 2014.

O'Rorke, R., Jeffs, A., Wang, M., Waite, A., Beckley, L., and Lavery, S.: Spinning in different directions: western rock lobster
larval condition varies with eddy polarity, but does their diet?, J. Plankton Res., 37, 542–553,
https://doi.org/10.1093/PLANKT/FBV026, 2015.

705   Pattiaratchi, C. and Buchan, S.: Implications of long-term climate change for the Leeuwin Current, J. R. Soc. West. Aust., 74,
133–140, 1991.

Pattiaratchi, C. and Hetzel, Y.: Sea surface temperature variability: State and trends of Australia's oceans report, Hobart, 1.2.1–
1.2.4 pp., 2020.

Pattiaratchi, C. and Siji, P.: Variability in ocean currents around Australia: State and trends of Australia's oceans report, Hobart,
710   1.4.1-1.4.6 pp., 2020.

Pattiaratchi, C. and Woo, M.: The mean state of the Leeuwin Current system between North West Cape and Cape Leeuwin, J.
R. Soc. West. Aust., 92, 221–241, 2009.

Pattiaratchi, C., Hegge, B., Gould, J., and Eliot, I.: Impact of sea-breeze activity on nearshore and foreshore processes in
southwestern Australia, Cont. Shelf Res., 17, 1539–1560, https://doi.org/10.1016/S0278-4343(97)00016-2, 1997.

715   Pawlowicz, R.: M_Map: A mapping package for MATLAB, Version 1.4m, 2020.

Pearce, A. and Griffiths, R.: The mesoscale structure of the Leeuwin Current: a comparison of laboratory models and satellite

imagery, J. Geophys. Res., 96, https://doi.org/10.1029/91jc01712, 1991.

Pearce, A. and Pattiaratchi, C.: The Capes Current: A summer countercurrent flowing past Cape Leeuwin and Cape Naturaliste, Western Australia, Cont. Shelf Res., 19, 401–420, https://doi.org/10.1016/S0278-4343(98)00089-2, 1999.

720   Pearce, A. and Phillips, B.: Enso events, the leeuwin current, and larval recruitment of the western rock lobster, ICES J. Mar. Sci., 45, 13–21, https://doi.org/10.1093/icesjms/45.1.13, 1988.

Phillips, B.: The circulation of the southeastern Indian Ocean and the planktonic life of the western rock lobster, Oceanogr. Mar. Biol. An Annu. Rev., 19, 11–39, https://doi.org/10.1071/MF9810417, 1981.

Phillips, B.: Prediction of Commercia Catches of the Western Rock Lobster (*Panulirus cygnus*), Can. J. Fish. Aquat. Sci., 43,

725   2126–2130, 1986.

Rennie, S., Pattiaratchi, C., and Mccauley, R.: Eddy formation through the interaction between the Leeuwin Current , Leeuwin Undercurrent and topography, Deep. Res. Part I Oceanogr. Res. Pap., 54, 818–836, https://doi.org/10.1016/j.dsr2.2007.02.005, 2007.

Säwström, C., Beckley, L., Saunders, M., Thompson, P., and Waite, A.: The zooplankton prey field for rock lobster phyllosoma

730   larvae in relation to oceanographic features of the south-eastern Indian Ocean, J. Plankton Res., 36, 1003–1016, https://doi.org/10.1093/plankt/fbu019, 2014.

Schiller, A., Oke, P., Brassington, G., Entel, M., Fiedler, R., Griffin, D., and Mansbridge, J.: Eddy-resolving ocean circulation in the Asian-Australian region inferred from an ocean reanalysis effort, Prog. Oceanogr., 76, 334–365, https://doi.org/10.1016/j.pocean.2008.01.003, 2008.

735   Smith, R., Huyer, A., Godfrey, S., and Church, J.: The Leeuwin Current off Western Australia, 1986-1987, J. Phys. Oceanogr., 21, 323–345, https://doi.org/10.1175/1520-0485(1991)021<0323:TLCOWA>2.0.CO;2, 1991.

Wang, M., O'Rorke, R., Waite, A., Beckley, L., Thompson, P., and Jeffs, A.: Condition of larvae of western rock lobster (Panulirus cygnus) in cyclonic and anticyclonic eddies of the Leeuwin Current off Western Australia, Mar. Freshw. Res., 66, 1158–1167, https://doi.org/10.1071/MF14121, 2015.

740   Wernberg, T., Smale, D., Tuya, F., Thomsen, M., Langlois, T., de Bettignies, T., Bennett, S., and Rousseaux, C.: An extreme climatic event alters marine ecosystem structure in a global biodiversity hotspot, Nat. Clim. Chang., 3, 78–82, https://doi.org/10.1038/nclimate1627, 2012.

Wickham, H., Francois, H., and Muller, K.: dplyr: A Grammar of Data Manipulation. R package version 0.7.6, 2018.

Wijeratne, S., Pattiaratchi, C., and Proctor, R.: Estimates of surface and subsurface boundary current transport around

745   Australia, J. Geophys. Res. Ocean., 123, 3444–3466, https://doi.org/10.1029/2017JC013221, 2018.

Wijffels, S., Beggs, H., Griffin, C., Middleton, J., Cahill, M., King, E., Jones, E., Feng, M., Benthuysen, J., Steinberg, C., and Sutton, P.: A fine spatial-scale sea surface temperature atlas of the Australian regional seas (SSTAARS): Seasonal variability and trends around Australasia and New Zealand revisited, J. Mar. Syst., 187, 156–196, https://doi.org/10.1016/j.jmarsys.2018.07.005, 2018.

750   Woo, M. and Pattiaratchi, C.: Hydrography and water masses off the western Australian coast, Deep. Res. Part I Oceanogr.

Res. Pap., 55, 1090–1104, https://doi.org/10.1016/j.dsr.2008.05.005, 2008.

Wood, S. N.: Generalized Additive Models: An Introduction with R, Second Edition, CRC Press, 2017.

Yeung, C., Jones, D., Criales, M., Jackson, T., and Richards, W.: Marine freshwater influence of coastal eddies and countercurrents on the influx of spiny lobster , Mar. Freshw. Res., 52, 1217–1232, 2001.

755

760